Food Hydrocolloids 110 (2021) 106132

Contents lists available at ScienceDirect

Food Hydrocolloids

journal homepage: http://www.elsevier.com/locate/foodhyd

Towards recombinantly produced milk proteins: Physicochemical and emulsifying properties of engineered whey protein beta-lactoglobulin variants

Julia K. Keppler [a,b,*], Anja Heyse [c], Eva Scheidler [d], Maximilian J. Uttinger [e], Laura Fitzner [b], Uwe Jandt [f,g], Timon R. Heyn [b], Vanessa Lautenbach [e], Joanna I. Loch [h], Jonas Lohr [i,j,k], Helena Kieserling [l], Gabriele Günther [k,m], Elena Kempf [i,j,k], Jan-Hendrik Grosch [i,j,k], Krzysztof Lewiński [h], Dieter Jahn [k,m], Christian Lübbert [e], Wolfgang Peukert [e], Ulrich Kulozik [d], Stephan Drusch [c], Rainer Krull [h,i,j], Karin Schwarz [b], Rebekka Biedendieck [k,m]

[a] Wageningen University, Laboratory of Food Process Engineering, P.O. Box 17, 6700 AA, Wageningen, the Netherlands
[b] Kiel University, Division of Food Technology, 24118, Kiel, Germany
[c] Technische Universität Berlin, Chair of Food Technology and Food Material Science, Straße des 17. Juni 135, 10623 Berlin, Germany
[d] TU Munich, Chair of Food and Bioprocess Engineering, Weihenstephaner Berg 1, 85354, Freising, Germany
[e] Friedrich-Alexander-Universität Erlangen-Nürnberg, Institute of Particle Technology, Interdisciplinary Center for Functional Particle Systems, Haberstraße 9a, 91058 Erlangen, Germany
[f] Hamburg University of Technology, Bioprocess and Biosystems Engineering, Hamburg, Germany
[g] Deutsches Elektronen-Synchrotron DESY, Information Technology, Notkestrasse 85, 22607, Hamburg, Germany
[h] Jagiellonian University, Faculty of Chemistry, Gronostajowa 2, 30-387 Kraków, Poland
[i] Technische Universität Braunschweig, Institute of Biochemical Engineering, Rebenring 56, 38106, Braunschweig, Germany
[j] Technische Universität Braunschweig, Center of Pharmaceutical Engineering (PVZ), Franz-Liszt-Straße 35a, 38106, Braunschweig, Germany
[k] Technische Universität Braunschweig, Braunschweig Integrated Centre of Systems Biology (BRICS), Rebenring 56, 38106, Braunschweig, Germany
[l] Technische Universität Berlin, Chair of Food Colloids, Straße des 17. Juni 135, 10623 Berlin, Germany
[m] Technische Universität Braunschweig, Institute of Microbiology, Rebenring 56, 38106, Braunschweig, Germany

1. Introduction

The growing world population and its increasing demand for high-quality protein will have a strong impact on future research topics. The production of animal proteins as sole protein source is not sustainable because it takes up enormous environmental impact with low production efficiency. Various approaches are already aimed at addressing these challenges: Alternative and sustainable sources such as plants, insects, fungi and bacteria are being tested for their natural amino acid value and protein yield (Dekkers, Boom, & van der Goot, 2018; Mishyna, Chen, & Benjamin, 2020; van der Weele, Feindt, van der Goot, van Mierlo, & van Boekel, 2019). In order to increase consumer

Abbreviations: BLG AB, bovine beta-lactoglobulin isoform AB mixture; BLG B, bovine beta-lactoglobulin isoform B; rBLG B, recombinant bovine beta-lactoglobulin isoform B with additional N-terminal M; sBLG B, recombinant bovine beta-lactoglobulin isoform B with N-terminal L1A/I2S substitutions; AUC, analytical ultracentrifugation; DLS, dynamic light scattering; DNPH, 2,4-dinitrophenylhydrazine; DiTyr, dityrosine; DTNB, 5,5-'Dithio-bis-(2-nitrobenzoic acid); DTT, Dithiothreitol; Gua-HCl, guanidine hydrochloride; OPA, o-phtalaldehyde; PMSF, phenylmethylsulfonylfluoride; PTM, post-translational modifications; NAC, N-acetyl-L-cysteine; NFK, N-formylkynurenine.

* Corresponding author. Wageningen University & Research, AFSG: Laboratory of Food Process Engineering, P.O. Box 17, 6700 AA Wageningen, Wageningen Campus, Building 118 (Axis), Bornse Weilanden 9, 6708 WG, Wageningen, the Netherlands.

E-mail addresses: julia.keppler@wur.nl (J.K. Keppler), anja.heyse@tu-berlin.de (A. Heyse), eva.scheidler@tum.de (E. Scheidler), max.uttinger@fau.de (M.J. Uttinger), lfitzner@foodtech.uni-kiel.de (L. Fitzner), uwe.jandt@tuhh.de (U. Jandt), theyn@foodtech.uni-kiel.de (T.R. Heyn), vanessa.lautenbach@fau.de (V. Lautenbach), loch@chemia.uj.edu.pl (J.I. Loch), j.lohr@tu-braunschweig.de (J. Lohr), helena.schestkowa@tu-berlin.de (H. Kieserling), g.guenther@tu-braunschweig.de (G. Günther), e.kempf@tu-braunschweig.de (E. Kempf), jan-hendrik.grosch@tu-braunschweig.de (J.-H. Grosch), lewinski@chemia.uj.edu.pl (K. Lewiński), d.jahn@tu-braunschweig.de (D. Jahn), christian.luebbert@fau.de (C. Lübbert), wolfgang.peukert@fau.de (W. Peukert), ulrich.kulozik@tum.de (U. Kulozik), stephan.drusch@tu-berlin.de (S. Drusch), r.krull@tu-braunschweig.de (R. Krull), info@foodtech.uni-kiel.de (K. Schwarz), r.biedendieck@tu-braunschweig.de (R. Biedendieck).

https://doi.org/10.1016/j.foodhyd.2020.106132
Received 22 March 2020; Received in revised form 8 June 2020; Accepted 24 June 2020
Available online 7 July 2020

acceptance, these proteins are also selected for their ability to mimic the texture and taste of meat or dairy products (Dekkers et al., 2018; Paul, Kumar, Kumar, & Sharma, 2019; Sethi, Tyagi, & Anurag, 2016).

Another approach is the possibility of *in vitro* farming (cellular agriculture). Recombinant production of chymosin for cheese making has been done for years (Tagliavia & Nicosia, 2019). Novel approaches are the *in vitro* production of meat via tissue engineering (Bhat, Kumar, & Fayaz, 2015). Further, there is potential interest in recombinantly produced dairy proteins (Vestergaard, Chan, & Jensen, 2016). The commercial and environmental sustainability of these recombinantly produced proteins/products at a scale relevant for feeding the world population has still to be proven. In order to clarify the challenges and opportunities of this emerging technology, it is of great importance to investigate the production processes and functional equivalence of recombinant proteins.

The production of recombinantly produced whey protein beta-lactoglobulin (BLG) is particularly interesting in this respect, as it is the main protein in bovine whey and as such an important component in many foods. It also has versatile functional properties, e.g. as gelling, foaming and emulsifying agent (Dombrowski, Gschwendtner, Saalfeld, & Kulozik, 2018; Keppler, Steffen-Heins, Berton-Carabin, Ropers, & Schwarz, 2018; Lam & Nickerson, 2014). Since BLG is also a central model protein in structural biology, several efforts for its recombinant production have been published. It exists predominantly in two isoforms (BLG A and BLG B) in bovine milk, which differ by two amino acids. Many studies focused on BLG A or B production in yeasts (Denton et al., 1998; Kim et al., 1997; Yagi, Sakurai, Kalidas, Batt, & Goto, 2003), which resulted in a high yield but either contained several changes in the N-terminal region of BLG and/or led to co-produced (poly)saccharides. The latter can interact with BLG and lead to structural changes as well as protein-protein interactions (Hundschell, Bäther, Drusch, & Wagemans, 2020). Yeast-based production and commercial application of recombinant BLG for food products are described in patent US9924728B2 et al. (2018) and Perfect Day Inc. started to commercialize. The company admits that their product may exhibit post-translational modification (PTM) in the form of glycozylation, which is typical for proteins recombinantly produced in eukaryotes.

However, a correctly folded protein with high amino acid availability, preserved functionality, and solubility is essential to replace the natural BLG in a broad range of food applications. Batt, Rabson, Wong, and Kinsella (1990) proposed the intracellular production of BLG in *Escherichia coli* (*E. coli*) as a prelude for potential structure/function related research through site-directed mutagenesis, which initially led to insoluble protein. Ponniah and colleagues finally succeeded in producing correctly folded soluble BLG B in *E. coli* (Ponniah et al., 2010) still carrying the N-terminal start methionine (rBLG B) which is missing in the native bovine BLG B. This variant has recently been further improved by Loch et al. by introducing a L1A/I2S mutation (sBLG B) to ensure correct cleavage of the N-terminal methionine (Loch et al., 2016), which was suitable for ligand binding studies. In addition, protein isolation from the microorganism has been optimized to remove the endogenous fatty acids that were bound in the hydrophobic protein pocket after protein production as well as to ensure high purity and nativity. The crystal structure and conformation of the recombinant sBLG B (PDB ID: 6QI6) produced in this way is very similar to that of the natural bovine BLG B (PDB ID: 3NPO), isolated from bovine milk (Loch et al., 2016) and the recombinant protein was considered suitable for biochemical studies.

Now it is also of interest to study the possibility to use these proposed genetically engineered BLGs from *E. coli* with respect to possible food applications. Here, a recombinant wild type BLG B variant still carrying a methionine at its N-terminus (rBLG B) but without any further amino acid mutations as well as a recombinant BLG B variant with L1A/I2S modification (sBLG B) for accurate N-terminal cleavage of the methionine proposed by Loch et al. (2016) were produced in *E. coli* and purified with an adapted protocol. The physicochemical and emulsifying properties of the recombinant variants were compared with those of commercial BLG B isolated in high purity from bovine milk. In addition, isolated BLG AB was chosen as reference, because this mixed variant is present in all food-related BLG formulations. Similar emulsifying properties (in the range of commercial BLG B and isolated BLG AB) are an important prerequisite for the substitution of bovine BLG with recombinant BLG in many food products.

Our approach is new and unique in that it investigates how the necessary/unavoidable N-terminal modifications of the recombinant BLG variants affect their physicochemical and functional properties in the context of potential food applications, in particular, their emulsion-forming capacity. This work differs from previous work in the field as it is intended to investigate whether the emulsion forming ability of the recombinant variants is equivalent to that of BLG isolated from bovine milk while many previous studies with recombinant BLG rather focused on structure/functionality effects of cysteine 121 mutagenesis or addition of a third disulphide bond (Jayat et al., 2004; Cho et al., 1994). The working hypothesis of the present investigations is that the small structural changes that were necessary/unavoidable for the expression of a correctly folded recombinant BLG B in *E. coli* might modify some physicochemical properties but not affect its functionality (*i.e.*, emulsifying properties) in the final product.

The results presented here provide the possibility of a better understanding of the behavior of the genetically modified BLG variants under processing induced stress and their functionality compared to those of native bovine BLG. This manuscript also gives a comprehensive overview of the physicochemical properties of different BLG variants, modeled or measured with a large variety of current methods, as well as insights into the functionality of two different recombinant variants with specific single amino acid changes. This provides the basis for evaluating the substantial equivalence of the recombinant variants as a prerequisite for approval in the food industry. It also allows the selection of the most suitable recombinant variant for potentially high-yield production also in other bacteria than *E. coli*, to eventually be used in food products. In the future, such results may contribute to the assessment of economic and ecological sustainability of this concept.

2. Materials & methods

2.1. Materials

The recombinant BLG B variants were produced and isolated as described further below. Commercial protein BLG B (L8005, isolated from bovine milk) was purchased from Sigma Aldrich (Steinheim, Germany). Bovine BLG AB was isolated from bovine milk according to Toro-Sierra, Tolkach, and Kulozik (2013). 5,5-'Dithio-bis-(2-nitrobenzoic acid) (DTNB), o-phtalaldehyde (OPA), 2,2-Bis(hydroxymethyl)-2,2′,2″-nitrilo-triethanol, L-leucine, Dithiothreitol (DTT), 2, 4-dinitrophenylhydrazine (DNPH) and phenylmethylsulfonylfluoride (PMSF) were purchased from Sigma Aldrich (Steinheim, Germany). Boric acid, glycine, N-acetyl-L-cysteine (NAC), Tris, sodium hydroxide (NaOH), o-phosphoric acid (85%), acetonitrile (ACN), guanidine hydrochloride (Gua-HCl), trifluoroacetic acid (TFA), trisodium citrate, hydrochloric acid (HCl, 37%) and Florisil (activated magnesium silicate; $MgO \cdot 3.6\ SiO_2 \cdot 1.53$ OH, 100%) was from Carl Roth (Karlsruhe, Germany), Merck (Darmstadt, Germany), and/or Sigma Aldrich (Steinheim, Germany). Benzonase (250 U/μL) was purchased from Merck (Darmstadt, Germany). Ethanol and ethyl acetate were from VWR (Radnor, USA). Middle-chain triacylglyceride oil (Witarix MCT 60/40, >99.9%) was purchased from IOI Oleochemical (Hamburg, Germany). All chemicals were of analytical grade. For all experiments, ultrapure water ($\leq$18.2 MΩ cm^{-1}) was used. Borosilicate membranes (type P4) were purchased from ROBU Glasfilter-Geräte (Hattert, Germany).

2.2. Sample preparation

Unless otherwise stated, protein solutions were prepared by dissolving 10 mg/mL commercial BLG B, isolated bovine BLG AB, or one of the two recombinant variants rBLG B and sBLG B in ultra-pure water. After stirring the protein solutions for at least 1 h, the pH value was set to pH 7 using NaOH.

2.3. Production and purification of recombinant BLG

2.3.1. Recombinant production

For the production of recombinant bovine BLG B, *E. coli* Origami B (DE3) cells (Novagen, Darmstadt Germany) were transformed with the plasmids pETDuet-1/DsbC/BLGB (encoding recombinant beta-lactoglobulin isoform B, denoted as "rBLG B″) and pETDuet-1/DsbC/L1A/I2S-BLGB (encoding recombinant beta-lactoglobulin isoform B with modified N-terminus L1A/I2S, denoted as "sBLG B″), respectively, as described previously (Loch et al., 2016). Recombinant cells were grown in 50 mL LB-medium supplemented with 100 μg/mL carbenicillin and 2 g/L glucose at 37 °C and 150 min^{-1} overnight. 44 mL of this culture were added to 1 L LB-medium supplemented with 100 μg/mL carbenicillin and 2 g/L glucose in a 2 L baffled shaking flask and incubated until reaching an OD_{600} of 0.5–0.7 (pETDuet-1/DsbC/BLGB) and 1.0–1.2 (pETDuet-1/DsbC/L1A/I2S-BLGB), respectively. Recombinant protein production was induced by adding 500 μM isopropyl-β-D-thiogalactopyranosid (IPTG, Sigma-Aldrich). After incubation for 4 h (pETDuet-1/DsbC/BLGB) and overnight (pETDuet-1/DsbC/L1A/I2S-BLGB), respectively, at 25 °C and 140 min^{-1}, cells were harvested at 4 °C (20 min, 3000 g), resuspended in 20 mL sodium phosphate buffer (20 mM, pH 6), harvested again at 4 °C (40 min, 3000 g) and stored at −80 °C. 1 L cell culture resulted in approximately 4.5–8 g of wet cells.

2.3.2. Purification

For the purification of recombinant BLG B variants, 30 mL sodium phosphate buffer (20 mM, pH 6) was added and cells were thawed on ice, resuspended, and supplemented with 15 μL PMSF (200 mM) and 0.15 μL benzonase (250 U/μL) per 30 mL. Cells were disrupted by sonication for 4 · 5 min, with 5 min gaps between (settings: 97% power, 5 · 10% cycles). Disrupted cells were transferred into 2 mL reaction vials and centrifuged for 90 min at 18,000 g and 8 °C. The supernatant was filtrated (pore size of 0.45 μm). Before loading the filtrated cell lysate (around 3000 mg total protein) on a HiTrap Capto Q ImpRes chromatography column (10 mL column volume; GE Healthcare Life Sciences, Chicago, USA), the anion exchange column was equilibrated with sodium phosphate buffer (20 mM, pH 6). Proteins were eluted using a linear gradient from zero to 500 mM NaCl (20 column volumes). Fractions containing the highest amount of recombinant BLG B were combined, adjusted to 1.5 M of ammonium sulfate, incubated overnight at 4 °C and centrifuged for 20 min at 2900 g and 4 °C. 7.5 mL of the supernatant containing BLG B was loaded on a HiPrep desalting 26/10 column (53 mL column volume; GE Healthcare Life Sciences, Chicago, USA) and eluted using ultrapure water. Finally, proteins were lyophilized for 62 h using a temperature gradient from −35 °C to 25 °C (Beta 2–8 LSCplus, Martin Christ, Osterode am Harz, Germany). Vials containing lyophilized BLG B were closed under dry nitrogen atmosphere and stored at 4 °C. All chromatographic purification steps were carried out using the Äkta Pure 150 (GE Healthcare Life Sciences, Chicago, USA) fast protein liquid chromatography system. Throughout the whole purification process, protein fractions were analyzed by SDS-PAGE (12% (w/v) of acrylamide) as described before (Righetti, 1990).

2.4. Sequence and structure analyses

BLG concentrations were measured by NanoDrop microvolume spectrophotometer (Peqlab Biotechnology GmbH, Erlangen, Germany). In addition, the percentage of the BLG protein band in comparison to all bands was calculated from the SDS-Page images using GelAnalyzer software (version 19.1, free software, GelAnalyzer.com). The N-terminal amino acid sequence of the recombinant variants was analyzed by automatic Edman degradation (Edman & Begg, 1967).

2.4.1. Analysis of covalent protein modifications

Mass spectrometry was conducted to screen for acetylation, glycozylation, or other covalent protein modifications occurring in bovine milk or during recombinant production. In addition, mass shifts reveal changes in the amino acid sequence. For the analysis of the protein samples a Qq-TOF (Bruker, Impact II, Resolution 40.000) with ion-mobility analysis (Seadm, differential mobility analysis, DMA, Resolution 60) was used.

2.4.2. Molecular dynamic analysis

The BLG variants were analyzed using molecular dynamics (MD), which gives information on the dynamic properties of the protein variants. All MD simulations and analyses were performed using the GROMACS software package version 5.1.1 (Van Der Spoel et al., 2005) and the OPLS-AA (all-atom) force field (Kaminski, Friesner, Tirado-Rives, & Jorgensen, 2001). The structure of native dimeric BLG has been obtained from PDB 3PH5. The original structure misses a few N-terminal amino acids, *i.e.*, it starts at a position denoted there as number 20 (TQTMK–; *c.f.* Table 1). The remaining N-terminal amino acids for all variants (BLG A or B: LIV–; rBLG B: MLIV–; sBLG B: ASV–) were added

Table 1
Sequence and structure properties of BLG variants used within this study.

Name	BLG AB	BLG B	rBLG B	sBLG B
Purity (Nanodrop) [%]	>90	>90	>90	>90
Sequence of N-Terminus	LIVTQ	LIVTQ	**M**LIVTQ	**AS**VTQ
Length [amino acids]	162	162	163	162
Calculated molecular weight [Da] [1]	18,366.27	18,280.17	18,411.36	18,211.99
MS measured molecular weight [Da] [1]	18,374.9	18,288.9	18,419.9	18,220.9
MS measured mass difference to BLG B [Da] [1]	+86	0	+131	−68
Measured SH groups [mol/mol protein]	0.43 ± 0.0[b,c]	0.35 ± 0.0[a]	0.45 ± 0.0[c]	0.38 ± 0.0[a,b]
Measured NH groups [mol/mol protein]	19.6 ± 0.5[b]	17.6 ± 1.0[a,b]	17.0 ± 0.1[a]	16.7 ± 0.6[a]
Measured isoelectric point (IEP)	4.9 ± 0.12	4.7 ± 0.20	5.4 ± 0.05	5.4 ± 0.08
Theoretical IEP calculated for unfolded BLG [1]	4.76	4.83	4.83	4.83
Acid solubility [%]	98 ± 0.6[a]	88 ± 0.4[c]	96 ± 0.3[b]	97 ± 0.5[a,b]
MD simulations				
MD root mean squared deviation, all atoms [nm]	n. d.	0.29 ± 0.022[a]	0.36 ± 0.068[b]	0.29 ± 0.022[a]
MD radius of gyration of monomer [nm]	n. d.	1.53 ± 0.013[a]	1.54 ± 0.016[a]	1.52 ± 0.013[a]
MD SASA of single monomers [nm^2]	n. d.	178.9 ± 1.4[a]	183.0 ± 1.75[b]	178.5 ± 1.53[a]
MD SASA of dimer [nm^2]	n. d.	166.2 ± 1.0[a]	168.9 ± 1.10[b]	165.6 ± 1.01[a]
MD intramolecular H-bonds of monomer	n. d.	224 ± 3.1[a]	225 ± 3.7[a]	223 ± 3.0[a]
MD intramolecular H-bonds of dimer	n. d.	231 ± 4.8[a]	232 ± 4.3[a]	234 ± 3.4[a]

[1] Properties of BLG A are listed instead of BLG AB for some instances where only monomer structure was assessed. Significant differences in a row ($p < 0.05$) are indicated by small letters (a-c). MD simulations of BLG AB were not determined (n. d.) because of its presence as a homodimer (AA or BB) or heterodimer (AB) in a mixture at pH 7. H-bonds, hydrogen bonds; MD, molecular dynamics; MS, mass spectrometry; SASA, solvent accessible surface area.

using Modeller V9.15 (Marti-Renom et al., 2000). The resulting models were equilibrated and simulated as described in Uttinger et al. (2020). The temperature was maintained at T = 293 K, pH was set neutral and salt concentration was set to 10 mM. Two types of simulations were performed subsequently: First, 5 ns of free (unforced) simulation was conducted (*MD-free*), followed by 0.7 ns of forced simulation, separating the two monomers along the dimer's principal axis by pulling with constant velocity ($v = 5\ ms^{-1}$) and adapted force (*MD-pull*). Root mean squared deviations of respective structures (RMSD), radius of gyration (R_g), surface accessible area (SASA), hydrogen bonds binding energies were extracted for all simulations and pulling forces from the *MD-pull* simulations using the respective GROMACS (GROningen MAchine for Chemical Simulations) tools. Each simulation was repeated independently, yielding $n = 20$ replicates for each variant, thus total 120 simulations. Comparison of extracted data between variants allowed for statistical significance testing (Student's two-sided *t*-test) and calculation of confidence intervals (p = 95%, assuming normal distribution).

2.4.3. Analysis of free thiol group reactivity (RSH test)

The number of accessible thiol groups (SH groups) per protein was determined according to a variation of the Ellman's assay (Ellman, 1959) without denaturing conditions as reported previously (Keppler et al., 2014). 1.6 mL tris-glycine buffer (50 mM, pH 8.5), 400 μL BLG solution, and 40 μL DTNB (10 mM in 50 mM tris-glycine buffer, pH 8.5) were mixed and incubated for 10 min at room temperature. The absorbance of the mixture was measured at 412 nm using a spectrophotometer (Helios Gamma, UV–Vis, Thermo Spectronic, Cambridge, UK). The concentration of free thiol groups, expressed as free thiol groups per protein molecule, was determined using the molar attenuation coefficient of 13,600 $M^{-1}cm^{-1}$. All results were corrected for the protein concentration which was determined by measuring the absorbance of the supernatant at 278 nm after centrifugation using a molar extinction coefficient of 17,600 $M^{-1}cm^{-1}$.

2.4.4. Analysis of free amino groups (NH groups)

The amount of accessible amino groups on the different BLG variants was measured with the o-phtalaldehyde (OPA) method. BLG concentrations were set to 3.33 mg/mL (~180 μM). Due to poor solubility, rBLG B was centrifuged for 5 min at 4000 g and 20 °C. All results were corrected for the protein concentration which was determined by measuring the absorbance of the supernatant at 278 nm using a molar extinction coefficient of 17,600 $M^{-1}cm^{-1}$.

The determination of free amino groups was performed according to Roth (Roth, 1971) with slight modifications. In the presence of reduced thiol groups, OPA reacts with free amino groups by forming a fluorophore. 120 μL protein solution was mixed with 2.64 mL NAC (18.4 mM) in borate buffer (100 mM, pH 9.3) and 150 μL ultra-pure water instead of a denaturing agent. The mixture was incubated at 50 °C for 10 min. After the addition of 90 μL OPA (250 mM) the mixture was further incubated at 50 °C for 30 min. The final protein concentration was approximately 5 μM. The mixture was cooled down to room temperature for 30 min and the absorbance was measured at 340 nm using a spectrophotometer (Helios Gamma, UV–Vis, Thermo Spectronic, Cambridge, UK). For the calculation of the amount of free amino groups, a standard curve of L-leucine in a concentration range of 1.2–120 μM was used. The amount was expressed as the number of free amino groups per protein molecule.

2.4.5. Zeta potential and isoelectric point

The zeta potential is related to the net surface charge of the proteins and was measured using the Zetasizer instrument Nano ZS (Malvern Instruments, Herrenberg, Germany). The solutions were dialyzed against 10 mM NaCl solution for at least 4 h, and the dialysate was changed at least once to remove minor contamination. The pH of the protein solutions was adjusted with HCl and NaOH. BLG concentrations were set to 1.0 mg/ mL (~60 μM). The samples were prepared using a similar 10 mM NaCl solution as used in dialysis in order to ensure constant ionic strength after dilution, which is important for the subsequent analytical ultracentrifugation (AUC) analysis for a determination of the dimer dissociation constants K_D. Finally, the protein concentrations were controlled again via UV/VIS spectroscopy (Analytic Jena, Specord 210, Jena, Germany). The pH was controlled directly before the measurements and adjusted accordingly using HCl and NaOH.

For the determination of the isoelectric point (IEP), different pH values were set between 2 and 11 with 100 mM NaOH and 100 mM HCl to determine the point where the zeta potential reaches 0. For all measurements, a folded-capillary cuvette (Malvern Instruments, Malvern, Grovewood, UK) was used. The temperature was controlled at 25 °C with an initial equilibration time of 120 s.

2.4.6. Acid solubility by HPLC

To determine the relative amount of correctly folded BLG of each variant, the reversed phase (RP)-HPLC method to determine whey proteins in cow's milk was applied, modified according to Dumpler, Wohlschläger, and Kulozik (2017). In brief, BLG concentrations were set to 1 mg/mL and stirred at room temperature for 4 h. To determine the native BLG content, the pH of the protein solutions was adjusted to 4.6 reaching the isoelectric point of denatured BLG, which facilitates their precipitation, while intact BLG remains soluble in the supernatant. The concentration of denatured BLG was calculated from the content in the supernatant relative to the amount in the original sample.

For analysis, 200 μL of each sample was mixed with 800 μL of buffer and incubated for 30 min at room temperature. The mixture was manually shaken to ensure the complete solubilization of proteins. Analysis was carried out using an Agilent 1100 series chromatograph (Agilent, Waldbronn, Germany) equipped with a Latek 300 Å PLRP-S-C18 (Agilent, Waldbronn, Germany) column and eluted with a gradient of the two eluents A and B. Eluent A contained 90% ultrapure water, 10% acetonitrile (ACN) and 0.1% trifluoroacetic acid (TFA), eluent B contained 10% ultrapure water, 90% ACN and 0.07% TFA. The RP-HPLC was performed with a flow rate of 1 mL/min with the following gradient of water and ACN: 0–2 min (43–47% B), 6–9 min (49–52% B), 11–13 min (54–55%), 13.5–13.8 min (100%) and 14 min (100–14% B). The injection volume was 20 μL. The temperature of the column was 40 °C. The proteins were detected by UV/Vis at a wavelength of 226 nm. The evaluation of chromatograms was performed using the Agilent ChemStation Software (Rev.B.04.03.). Experiments were performed in duplicate.

2.4.7. Conformation analysis by FTIR

Protein secondary structure was analyzed using ATR-Fourier transform infrared spectroscopy (FTIR) on a Confocheck™ Tensor II system (Bruker Optics, Ettlingen, Germany) optimized for protein analytics in solutions and a thermally controlled BioATR2 unit as previously described by Kayser, Arnold, Steffen-Heins, Schwarz, and Keppler (2020).

Measurements were conducted at a temperature of 25 °C against the respective solvent mixtures without protein as background and averaged over 120 scans at a resolution of 0.7 cm^{-1}. For evaluation, the measured spectra underwent atmospheric correction and were then vector-normalized. The second derivative of the amide band I (1590 - 1700 cm^{-1}) was calculated using nine smoothing points.

2.4.8. Conformation analysis by intrinsic tryptophan fluorescence

Conformational differences between the BLG variants were investigated using intrinsic tryptophan fluorescence. The analysis was conducted as previously described (Heyn et al., 2019): The intrinsic tryptophan fluorescence of centrifuged samples was carried out in quartz cuvettes using a Varian Cary Eclipse fluorescence spectrophotometer (Varian Darmstadt, Germany) with protein concentrations of 250 mg/mL. All measurements were performed at pH 7 with an

excitation of 295 nm. Emission spectra were collected between 310 and 404 nm. The results were corrected by the actual protein concentration, which was measured by the absorbance at 278 nm as described above.

2.5. Quaternary structure analysis

2.5.1. Molecular weight distribution in solution by analytical ultracentrifugation (AUC)

AUC follows the sedimentation velocity of proteins, which differ for different quaternary structures. BLG concentration series (0.25mg/mL to 1.5 mg/mL) were produced from a stock solution of 1.5 mg/mL . Therefore, BLG variants were dialyzed as described for zeta potential and IEP measurements.

A modified preparative centrifuge (Type Optima L-90 K, Beckman Coulter, Krefeld, Germany) was used for the sedimentation velocity (SV) AUC experiments. The experiments were performed at a fixed rotor speed of 50,000 min^{-1}. The temperature was set to 20 °C throughout the measurements. Titanium centerpieces with a path length of 12 mm were used for all experiments. The individual SV data, which are collected for each protein concentration and solution pH were analyzed with the continuous c(s)-model of the SEDFIT program to determine sedimentation coefficient distributions and the molar masses of the individual species (Brown & Schuck, 2006). Determination of the dimer dissociation constant K_D was conducted from a protein concentration series at preset pH of the solution and analysis of the respective sedimentation data was carried out via SEDANAL program (version 6.93) (Stafford & Sherwood, 2004). The equilibrium constant K_D is derived from the protein monomer-dimer equilibrium reaction and describes the ratio of association to dimers and dissociation to monomers. Further details are included in the supplementary. The partial specific volume for all BLG samples was set to 751 μL/g. The solvent properties were equivalent to the properties of water for all analysis steps. Concentration non-ideality effects are in these concentration ranges not interfering with these measurements (Uttinger et al., 2019).

2.5.2. Hydrodynamic diameter by dynamic light scattering (DLS)

In order to assess the hydrodynamic diameter of the different BLG variants, protein size was measured with a Zetasizer instrument (Nano ZS, Malvern Instruments, Herrenberg, Germany). Protein powders were solubilized in PBS (137 mM NaCl, 2.7 mM KCL, 10 mM Na_2HPO_4, 1.8 mM KH_2PO_4) at a concentration of 1 mg/mL in order to assure correct DLS analysis and the pH was adjusted to 7.0. The measurement was carried out at 20 °C. If necessary, protein solutions were filtered through a 0.45 μm cellulose filter. Then to track the particle size, 10 measurements were conducted. Each measurement was performed over a time span of 60 s. Measurements were carried out in backscattering mode at 173° to achieve the highest resolution for smaller particles. A refractive index of 1.45 was chosen and the solvent viscosity was assumed to be similar to water. The experiments were conducted in triplicate.

2.6. Physicochemical properties

2.6.1. Denaturation temperature by differential scanning calorimetry (DSC)

In order to determine the denaturation temperature of the proteins, differential scanning calorimetry was performed using a TA instruments Q 1000 series (TA instruments, Eschborn, Germany). BLG concentrations were set to 100 mg/mL (w/w) at pH 7 and incubated at room temperature for 4 h. Prior to the analysis, the instrument was equilibrated at 25 °C for 2 min. Then, the modulated (0.5 °C/min) ramp from 25 to 95 °C was started with a heating rate of 2 °C/min. After completing the ramp, the temperature was kept at 95 °C for 1 min. Experiments were performed in duplicate.

2.6.2. Protein hydrophobicity by HPLC

RP-HPLC was used as a measure of the protein hydrophobicity by applying a similar HPLC method as the one used for the acid solubility with minor variations: BLG concentrations were set to 1 mg/mL with ultra pure water and analyzed by RP-HPLC as previously described (Keppler et al., 2017). Shortly, RP-HPLC analysis was carried out on a Dionex Ultimate 3000 HPLC system (Thermo Fisher Scientific, Waltham, USA) equipped with a polymeric reversed phase column (PLRP-S, 300 Å, 8 μm, 150 · 4.6 mm, Agilent Technologies, Santa Clara, USA). The separation was performed using ultra pure water with 0.1% TFA as eluent A and ACN with 0.1% TFA as eluent B. The applied gradient was 0–1 min (35% B), 8 min (38% B), 16 min (42% B), 22 min (46% B), 22.5–23 min (100% B) and 23.5 min (35% B). The injection volume was 20 μL at a flow rate of 1 mL/min. The temperature of the column was 40 °C. The detection wavelength was 205 nm.

In addition, the samples were also analyzed in a reducing and denaturating buffer system (0.02 M DTT and 6 M Gua-HCl) using the same column, flow rate, and column temperature, but detection wavelength of 226 nm and slightly different eluents mixtures: Eluent A: 100% ultrapure water, 0.1% TFA and Eluent B: 20% ultrapure water, 80% ACN, 0.0555% TFA. The applied gradient was 0 min (43% B), 2 min (47% B), 6 min (49% B), 9 min (52% B), 11 min (54% B), 13 min, (55% B), 13.5–13.8 min (100% B) and 14 min, (43% B).

2.7. Protein oxidation (carbonyl content, NFK, dityrosine)

Protein oxidation can occur during protein purification from milk or bacterial suspension. Protein carbonyl content was analyzed as described by Levine et al. (1990) and Scheidegger, Pecora, Radici, and Kivatinitz (2010). BLG concentrations were set to 3.33 mg/mL (~180 μM). Due to poor solubility, the recombinant wild type (rBLG B) was centrifuged for 5 min at 4000 g and 20 °C. For each sample, two aliquots were taken and analyzed as pairs (A and B): The protein (2 mg) was precipitated in each sample using 1 mL TCA (20%) and harvested by centrifugation at 10,000 g and room temperature for 5 min. The supernatant was discarded. One mL DNPH (100 mM in 2 M HCl) was added to one precipitate (A) and 1 mL HCl (2 M) the other (B). After incubation in the dark for 1 h at room temperature, 800 μL TCA (20%) were added, the samples were vortexed and centrifuged at 10,000 g for 5 min. The precipitated proteins were washed 3 times with 1 mL ethyl acetate/ethanol (1:1, v/v) to remove unbound DNPH. Afterwards, the proteins were redissolved in 2 mL Gua-HCl (6 M with 0.5 M phosphoric acid, pH 2.5). The absorbance was measured at 370 nm using a UV–Vis Spectrophotometer (Helios Gamma, Thermo Spectronic, Cambridge, UK). Protein carbonyls were calculated using the molar attenuation coefficient of $2.2 \cdot 10^{-4}$ $M^{-1}cm^{-1}$ and were expressed as nanomoles of carbonyls per milligram protein. All results were corrected by the protein concentration which was determined by measuring the absorbance of the precipitated and resuspended sample at 278 nm and by use of the molar extinction coefficient of 17,600 $M^{-1}cm^{-1}$.

The presence of dityrosine (DiTyr) and N-formyl-kynurenine (NFK) in the protein solution at pH 7 with a protein concentration of 1 mg/mL were analyzed in quartz cuvettes using a fluorescence spectrophotometer (Varian Cary Eclipse, Varian, Darmstadt, Germany) as described by Scheidegger et al. (2010). For DiTyr and NFK measurements, an excitation wavelength of 325 nm and emission wavelengths of 410 and 435 nm were used, respectively.

2.8. Surface activity and emulsifying properties

2.8.1. Adsorption behavior and interfacial rheology

To determine the adsorption behavior of the different BLG variants as well as their interfacial rheology, drop tensiometry with an oil/water (O/W) system was conducted.

Medium-chain triacylglyceride oil (MCT-oil) was used as the organic phase. To remove free fatty acids and other interfacial active compounds, MCT-oil was treated with Florisil as previously described (Schestkowa et al., 2019). The adsorption behavior of BLG at the O/W

interface was carried out with the pendant drop method using the profile analysis tensiometer (PAT1M, Sinterface Technologies, Berlin, Germany) with a two-fluid needle system as described by Schestkowa et al. (2019). Shortly, an ultrapure water droplet with a profile area of 50 mm^2 was dosed with the outer needle into the MCT-oil in a quartz-glass cuvette. Then, 2 μL of the water droplet was exchanged with 2 μL of 20 mg/mL (2 wt%) BLG solution (prepared in ultrapure water) through the inner needle (resulting BLG concentration in the pendant drop was 0.1 wt%). The interfacial tension analysis of the single drop was performed for 0.5 h at 22 °C by extracting the droplet shape recorded with a high-speed camera. The migration of the BLG through the droplet is characterized by the *lag*-time and was calculated in accordance with Schestkowa et al. (2019).

After the drop aging of 0.5 h, a subsequent amplitude sweep ranging from 0.1 to 7% deformation was performed at a frequency of 0.01 Hz as described by Tamm and Drusch (2017). The elastic (storage) modulus E and viscous (loss) modulus E" were derived from E*, which was calculated from the oscillation cycles. For E' > E'', the interfacial film is predominantly elastic, while for E' < E", the interfacial film is predominantly viscous. The property of the interfacial film is a characteristic parameter for the interfacial stabilization of emulsions.

2.8.2. Emulsifying properties

A coarse oil-in-water emulsion was prepared by dispersing 5% (w/w) purified MCT-oil (dispersed phase) in a 1 mg/mL (0.1 wt% BLG solution (continuous phase), prepared with ultrapure water) using a rotor-stator homogenizer (Ultra Turrax T25 basic, 500 W power output, S25 KD-25 F dispersion tool, IKA, Staufen, Germany) at 6500 min^{-1} for 15 s. Then, the coarse emulsions were pushed through a silicate membrane (membrane diameter 10 mm, membrane height 2.0 ± 0.2 mm median pore diameter 10–16 μm) to produce a fine emulsion. A new membrane was used for each emulsification. The oil droplet size distribution (D10, D50, D90, cumulative distribution function Q_0) of the coarse and fine emulsion was measured with a laser scattered light spectrometer (Horiba LA-950, Retsch Technology, Haan, Germany; transmission range: 80–95% (R) and 70–90% (B), refractive index: 1.46). Each sample was analyzed in analytical triplets, and the mean average of the analytical triplet was used as one technical measurement. Individual aliquots of 10 mL of the fine emulsions were transferred into graduated test tubes to check the emulsion stability after 1, 2, 3, and 144 h (7 d) visually.

2.9. Statistics

If not stated otherwise, all sample solutions were prepared in triplicate. Statistical significance was determined by calculating a one-way analysis of variance (ANOVA) and by using Tukey's multiple comparisons test as a post-hoc test. A significance level of 5% was assumed. The tests were performed using GraphPad Prism (version 6.07, GraphPad Software, San Diego, USA) or Statgraphics (Statgraphics Technologies Inc., version 5.1, the Plains, Virginia, USA).

3. Results

3.1. Production and purification of recombinant beta-lactoglobulin B (BLG B)

Within this study, two different bovine beta-lactoglobulin isoform B proteins, rBLG B with an additional methionine residue at the N-terminus (PDB ID: 5K06) and sBLG B (PDB ID: 6QI6) with a substituted N-terminus L1A/I2S as described by Loch et al. (2016) were recombinantly produced and purified (Table 1 and Fig. 1 and Fig. S1).

The purification process developed here using anion exchange chromatography followed by an ammonium sulfate precipitation of further *E. coli* host proteins and subsequent desalting resulted in >90% purity of the corresponding protein (Fig. S1). During this newly developed procedure, the proteins were kept under innocuous conditions to avoid stressful pH values or long times of dialysis, which were described by Ponniah et al. (2010) before. With these newly developed production and purification protocol including the addition of glucose to the growth medium combined with an improved purification procedure applying salting-out instead of size exclusion chromatography, the total yield of purified BLG B was significantly increased from up to 40 mg described previously (Loch et al., 2016) to 160 mg from 1 L of bacterial culture maintaining a high purity.

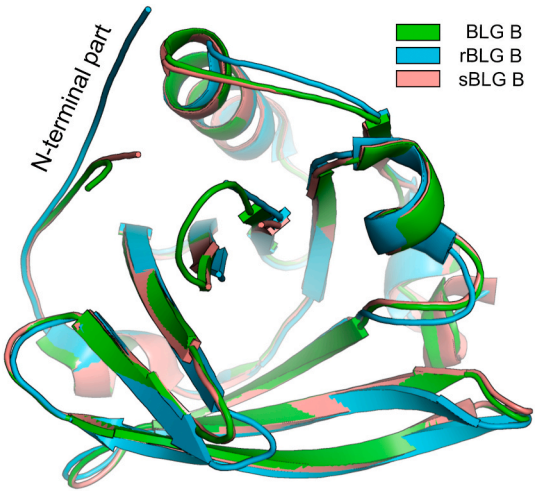

Fig. 1. Superposition (Cα) of lactoglobulin crystal structures: BLG B (PDB ID: 3NPO), rBLG B (PDB ID: 5K06) and sBLG B (PDB ID: 6QI6). The overall structure of all compared variants is almost the same but N-terminal part of the variant with additional N-terminal methionine (cyan) has different conformation than observed in natural protein isoform B (green) or a variant with N-terminal mutations L1A/I2S (pink). (For interpretation of the references to colour in this figure legend, the reader is referred to the Web version of this article.)

3.2. Properties of the BLG variants

Because of the changed production process, the proteins themselves were characterized in detail (e.g., N-terminal sequencing, mass spectrometry, thermal stability) to compare them with previously reported analyses by Loch et al. (2016). A number of additional analyses have been carried out that have not yet been done before with recombinant BLG (e.g. MD modeling, protein oxidation, dissociation constants by analytical ultracentrifugation).

3.2.1. Primary to tertiary structural properties of BLG variants

In the following, the two recombinant BLG B variants were compared to BLG B and BLG AB, which were isolated from bovine milk. All proteins used in this study had a purity higher than 90%. N-terminal sequencing proofed the differences in the N-termini of the recombinant proteins and the commercial BLG B. While rBLG B starts with methionine followed by leucine, isoleucine, and valine (Table 1, Fig. 1, Fig. S2), the starting methionine of sBLG B was missing due to cleavage during the recombinant production process as described before (Loch et al., 2016). Because of the introduced mutations supporting the N-terminal methionine cleavage *in vivo,* the first two amino acids in the mature sBLG B were found to be alanine and serine. No mixture of proteins with different N-termini could be found (Fig. S2).

Protein measurements by Qq TOF MS confirmed that covalent modifications of the proteins did not occur during production and purification processes. The deconvoluted signals at charge state +12 led to an expected molecular mass of 18,288.9 Da for the commercial BLG B sample, while sBLG B gave a 68 Da lower mass of 18,220.9 Da and rBLG B a higher mass of additional 131 Da (Table 1). The amount of accessible sulfhydryl groups (SH-groups) of the BLG variants can be used as a

measure of nativity or correct folding. With respect to the number of reactive thiol groups (determined in the RSH test), the present results show that both recombinant variants behave within the range of the bovine variants AB (0.43 mol/mol) and B (0.35 mol/mol), although rBLG B had a significantly higher thiol group accessibility than sBLG B (0.45 mol/mol and 0.38 mol/mol, respectively).

The amount of amino groups (NH groups, Table 1) of BLG variants gives an indication of covalent modifications (decrease of NH groups) or hydrolysis (increase of NH). Between 17 and 19.6 OPA (*o*-phtalaldehyde) amino groups could be observed for all BLG variants, with bovine BLG AB having the highest number of 19.6 detectable groups.

A significant difference in the measured isoelectric point (IEP) from 4.7 to 4.9 is evident between BLG B and BLG AB (Fig. S3). In addition to that, the recombinant BLG variants had a higher IEP than both reference proteins with 5.4, which could be caused by different ions present or some impurities because the theoretical IEP based on the unfolded amino acid chain for BLG B, sBLG B, and rBLG B are similar (IEP at pH 4.83). On the other hand, the IEP of unfolded BLG is generally lower than the IEP measured for native protein, with the exception of BLG B (Table 1). Such a difference between the IEP of native and denatured protein is only evident in some proteins due to specific amino acid composition and folding and caused by intramolecular amino acid interactions and lower solvent accessibility of buried amino acid groups in the native protein which can cause local charge differences (Ui, 1971).

The BLG acid solubility is a rough measure of its nativity and correct folding and is based on the lower IEP of unfolded BLG compared to native BLG (Table 1). Thus, denatured BLG precipitates at pH 4.6, while native BLG remains in solution. The BLG acid solubility was in the range of >96% for all proteins, which can be considered native. Again, the commercial protein BLG B deviated significantly from all other proteins with only 88% solubility (Table 1).

Molecular dynamic (MD) analysis of the three BLG B variants was performed to analyze structural differences in detail. Root mean squared deviations (RMSD) of monomers, whether in dimeric form or pulled apart in monomeric form, was slightly higher for rBLG B compared to combined sBLG B and BLG B: 0.36 ± 0.068 nm vs. 0.29 ± 0.022 nm; $p < 0.02$. The higher fluctuation for rBLG B is presumably dominated by the elongated N-terminal that, in all variants, remains only loosely attached to the remainder of the protein, whether dimeric or monomeric. Correspondingly, the radius of gyration was at 1.544 ± 0.016 nm for rBLG B vs. 1.524 ± 0.0088 nm for combined sBLG B and BLG B with an overall marginally significant difference ($p < 0.08$).

This further corresponded to a different solvent accessible surface area (SASA). The SASA of single monomers is larger for rBLG B than for combined BLG B and sBLG B (183.0 ± 1.75 nm^2 vs. 178.7 ± 1.01 nm^2; $p < 10^{-3}$). In the dimeric state (calculated per monomer), the difference in the SASA remained, however on a lower level (168.9 ± 1.08 nm^2 vs. 165.6 ± 1.01 nm^2; $p < 2{\cdot}10^{-3}$) while commercial and sBLG B cannot be distinguished based on SASA. Pulling forces needed to monomerize dimers were indistinguishable for all variants. The same held true for monomer-monomer binding energy. The number of stabilizing intramolecular hydrogen bonds has been found to be indistinguishable for all BLG variants: A larger number of bonds was identified for the dimeric state (calculated as the intramolecular H-bonds per monomer) of all BLG variants together (*i.e.*, mean of 232 ± 2.4) vs. a mean value of 224 ± 1.9 for all BLG variants in the monomeric state, but no differences were found between BLG B, sBLG B or rBLG B.

Fourier transform infrared (FTIR) spectroscopy was conducted to identify differences in the secondary and tertiary structural levels between the different BLG variants. The typical conformation of natively folded BLG was evident for BLG B, *i.e.*, the dominant intensity in the 1630 cm^{-1} band (Fig. 2A), indicating intramolecular beta-sheets, a less dominant alpha-helix at 1655–1658 cm^{-1} and a second beta-sheet band at 1688 cm^{-1} (Keppler et al., 2017; Keppler, Martin, Garamus, & Schwarz, 2015; Panick, Malessa, & Winter 1999). The BLG AB likewise showed a typical spectrum in the ATR-FTIR analysis with minor

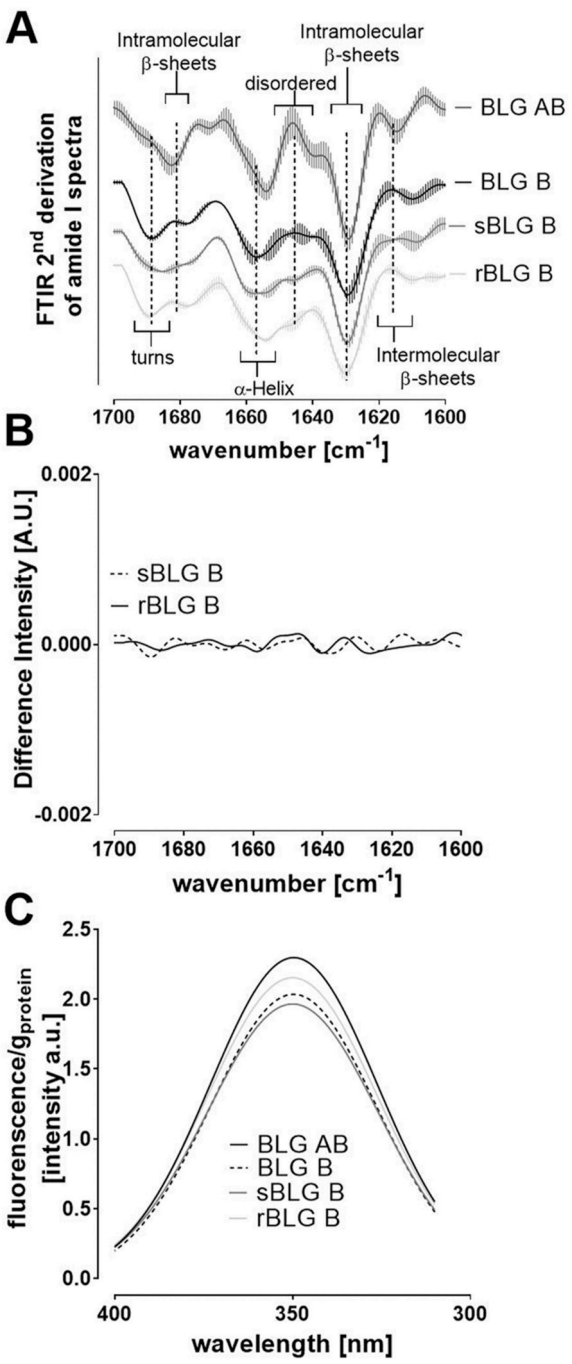

Fig. 2. A) ATR-FTIR second derivative amide I spectra of beta-lactoglobulin (BLG) variants. Waveband frequency regions for specific conformations (beta-sheets, helix, disordered) are indicated. **B)** FTIR amide I difference spectra between BLG B minus sBLG B or BLG B minus rBLG B. **C)** Intrinsic tryptophan fluorescence spectra between 300 and 400 nm emission for different BLG variants.

variances in the turns and disordered elements region compared to BLG B. There was also a minor band located at 1618 cm^{-1}, caused by intermolecular beta-sheets. The two recombinant variants sBLG B and rBLG B, however, exhibited a good resemblance to the BLG B spectrum, since the intensity difference spectra gave no strong deviations (<0.001 A.U.) (Fig. 2B).

The intrinsic tryptophan (Trp) fluorescence of BLG (Fig. 2C) is a sensitive measure of the accessibility of the aromatic amino acid Trp to the solvent. All BLG variants were again very similar in their

fluorescence intensity (approximately 1.8–2.3 A.U.) as well as emission wavelength maximum (approx. 350 nm wavelength). A slightly higher fluorescence intensity was observed for the BLG AB.

3.2.2. Quaternary structure

AUC can be used to analyze the sedimentation profile of a sample during centrifugation in real-time and it is thus possible to extract molecular size distributions in detail. The analysis of the monomer-dimer dissociation constant K_D of protein-protein interactions as a function of the pH value by AUC was first conducted with two samples (BLG AB and sBLG B) to determine the difference span (Fig. 3A). As can be seen, the K_D was almost similar for both tested variants. K_D decreased at pH 5 because of aggregation effects at the isoelectric point (IEP), while it increased towards more extreme pH values for both variants. Therefore, the remaining samples were measured only at one fixed protein concentration and at pH 7 and the monomer-dimer equilibrium was assessed based on these results.

The AUC results confirmed the predominant presence of dimers (36 kDa) for dialyzed BLG AB, sBLG B, and rBLG B at pH 7 in 10 mM NaCl, as well as some monomers (18.5 kDa) and multimers > 50 kDa (Fig. 3B). The small differences in the molecular weight of the different variants (Table 1) did not affect sedimentation and diffusional properties within sedimentation velocity (SV) AUC experiments. Moreover, the monomer-dimer equilibrium (Fig. 3A) was not different for the different BLG variants tested, hence the quaternary structure of the recombinant proteins has not been affected by the N-terminal modifications. Likewise, the hydrodynamic diameter measured in PBS using dynamic light scattering (DLS) gave the size of dimers between 5 and 6 nm, which was

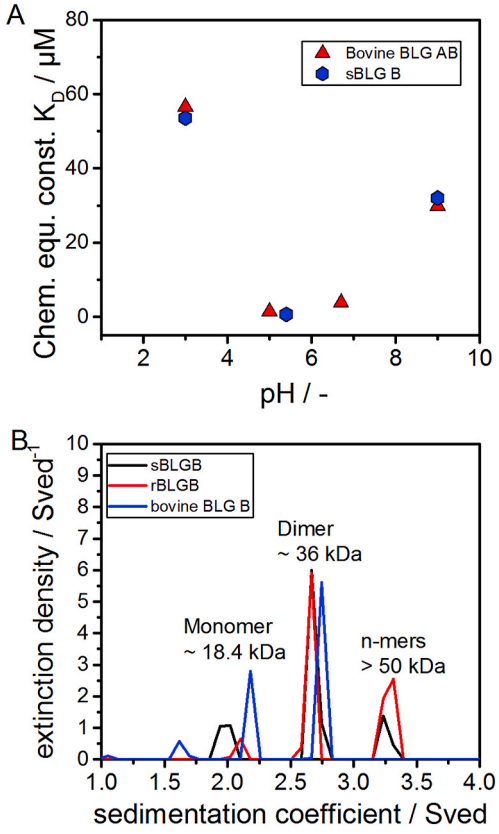

Fig. 3. A) Chemical equilibrium constant in terms of the dimer dissociation constant (K_D) derived from the monomer-dimer equilibrium of sBLG B and BLG AB as determined from SV AUC experiments at six different concentrations (0.25–1.5 g/L) in water set to pH values of 3, 5, 7 and 9. **B)** Sedimentation coefficient distribution as well as estimated molar masses from AUC data analysis for BLG B, sBLG B and rBLG B in water at pH 7 measured at a concentration of 1 g/L and rotor speed of 50,000 min^{-1}.

in accordance with results from AUC (Fig. 3, Table 2).

Zeta potential measurements (Table 2) showed minor differences between the reference proteins BLG AB and B (both −18.6 mV at pH 7) and the two recombinant variants (both - 21 mV).

3.2.3. Physicochemical properties

Different experiments were conducted to characterize the effect of the amino acid addition or substitution at the N-termini of the recombinant BLG B variants on their physicochemical properties compared to commercial BLG B and to BLG AB.

The denaturation onset temperature (T_d onset) of the natural bovine variants is an indication for the protein stability and its propensity to unfold, but also an important measure for its thermal stability during processing. T_d onset, as measured by differential calorimetry (DSC) (Fig. S4), was similar for both reference proteins with approximately 73 °C and increased significantly from BLG B to sBLG B by 1.7 K and from for BLG B and rBLG by 3.4 K. Protein denaturation was completed at higher temperatures between 77 °C for both reference proteins BLG B and BLG AB. The sBLG B showed a T_d less than 1 K higher, however, rBLG B differed by 3.2 K from BLG B.

Chromatographic separations according to protein hydrophobicity is shown in Fig. 4. The hydrophobicity of a protein is an important measure for its surface activity. The polarity of the protein decreases with increasing retention time (RT). While the BLG B eluted at 18.4 min, rBLG B eluted at 19 min and sBLG B at 17.8 min. The BLG AB reference confirmed that BLG B eluted at 18.4 min, while BLG A eluted at 19.5 min. When the proteins are completely unfolded (Fig. 4B) the hydrophobicity of initially hidden amino acids can be taken into account with this method. As can be seen, a similar elution order, albeit with a longer elution time difference is now evident. Due to the presence of Gua-HCL, however, all proteins elute now between 12 and 14 min (Fig. 4B) instead of 17 and 20 min (Fig. 4A).

3.3. Oxidation state

Protein oxidation that occurs during purification, processing, and storage of proteins, results in addition to post-translational modification in the organism to chemical modification of the BLG. Typical protein oxidation markers are protein-bound carbonyls detected by 2,4-dinitrophenylhydrazine (DNPH) derivatization as well as simple fluorescence measurements at Ex325nm/Em415nm and Ex325nm/Em435nm, which could be indicative for dityrosine oxidation (DiTyr) as a consequence of tyrosine oxidation and N-formylkynurenine formatione (NFK) as one of several tryptophan oxidation markers (Fig. 5) (Scheidegger et al., 2010).

The content of protein-bound carbonyls (Fig. 5A), however, is a reliable marker to assess the general oxidation state of proteins. All samples showed an overall low oxidation with respect to protein carbonyl (<1 nmol per mg of protein) or fluorescence formation (<30 Int A.U.). As NFK (Fig. 5B) and DiTyr (Fig. 5C) fluorescences showed overlap, the results could not clearly distinguish between Tyr or Trp oxidation. The results confirmed, that the recombinant production and isolation procedure had no detrimental effect on the oxidative state of the protein.

Table 2
Size and zeta-potential of all BLG variants used in this study.

	BLG AB	BLG B	rBLG B	sBLG B
Zeta Potential in 10 mM NaCl (pH 7) [mV]	−18.6 ± 1.2[a]	−18.7 ± 1.5[a]	−21 ± 0.6[a]	−21 ± 1.6[a]
Hydrodynamic diameter in PBS (pH 7) [nm]	5.4 ± 0.5[b]	5.2 ± 0.3[b]	5.4 ± 0.3[b]	6.0 ± 0.4[b]

[a] and [b]: significantly different values ($p < 0.05$) are indicated with different letters in a row.

Table 3
Characterization of all BLG variants used in this study.

	BLG AB	BLG B	rBLG B	sBLG B
T_d onset [°C]	73.0 ± 0.1[a]	73.3 ± 0.1[a]	76.7 ± 0.1[c]	75.0 ± 0.1[b]
T_d [°C]	77.5 ± 0.1[a]	77.3 ± 0.1[a]	80.5 ± 0.1[c]	78.2 ± 0.1[b]

T_d, denaturation temperature; [a] and [b]: significantly different values ($p < 0.05$) are indicated with different letters in a row.

3.4. Surface activity measurements

3.4.1. Interfacial tension

The dynamic interfacial tension curves (Fig. S5) give an indication of the propensity of a protein to unfold and align at a liquid interface and thus help to draw conclusions about its emulsifying properties. The curves were used to calculate the *lag*-time (*i.e.*, time until the first proteins adsorb and unfold at an interface), interfacial adsorption rate (*i.e.*, the velocity at which the interface is rearranged and occupied with proteins) and the equilibrium interfacial tension for stable systems (*i.e.*, the ability to stabilize the interfacial layer) (Table 4). The *lag*-times were similar with approximately 10 s for all variants except for the BLG AB mixture with 28 s.

In contrast, the adsorption rate of BLG AB was the highest (−1.05 mN $m^{-1}s^{-1}$) while BLG B exhibited the lowest rate with −0.12 mN $m^{-1}s^{-1}$. This could also be seen optically from the decrease of the interfacial tension (Fig. S6). The long-time equilibrium interfacial tension of the BLG B was also significantly higher (~20 mN $m^{-1}s^{-1}$) compared to the other BLG variants (~15 mN $m^{-1}s^{-1}$). When comparing only the recombinant variants, they showed no significant differences in their surface-active properties. They could be ranked between the BLG B and BLG AB samples.

Amplitude sweeps were used to investigate the physical properties of the protein layers at the O/W interface (Fig. S6). The dilatational elastic (E') and viscous (E") moduli were plotted as a function of the applied deformation of 0.8, 3.5, and 7%. All BLG films at the oil-water (O/W) interface exhibited viscoelastic properties (E'>E") (Fig. 6) with minor variations. The sBLG B film showed significantly lower elastic modulus E', which correlates to less elastic properties in the film compared to bovine BLG B and AB, while the rBLG B was in between (sBLG B < rBLG B < BLG B).

3.4.2. Emulsion oil droplet size

The mean emulsion oil droplet size of all proteins in the premix as well as in the final emulsion was not significantly different between the recombinant and the bovine variants (Fig. 7), except for the D90 sizes of the BLG B and rBLG B stabilized emulsion which were slightly larger than the D90 sizes of BLG AB and sBLG B. The fine emulsions produced by premix membrane-emulsification, where the resulting droplet size is determined by the used membrane pore size (10–16 μm), showed mean oil droplet sizes of approximately 13 μm size. In addition, also the creaming of the BLG stabilized emulsions (fine emulsions stored for 7 days) showed no differences and no separation of the dispersed phase (data not shown).

4. Discussion

The experiments were conducted to investigate how the single amino acid changes in the sequence of BLG variants affect the protein structure, physicochemical properties and finally, the emulsifying properties.

4.1. Structural properties

The BLG B variants differ in their N-terminal region, which affects the calculated and measured molecular weight. The lower mass of the sBLG B mutant compared to BLG B can be explained by the amino acid exchanges at positions 1 and 2 (Table 1, Fig. 1), which confirms a theoretical mass difference of −68 Da. In contrast, the additional methionine at the N-terminus of rBLG B adds 131 Da to the protein mass. Similar findings for rBLG B have been described in the literature (Loch et al., 2016).

Approximately 16 amino groups (*i.e.*, 15 epsilon-lysines and the N-terminal alpha amino group) can ideally be measured within native BLG A or B (Chevalier, Chobert, Popineau, Nicolas, & Haertlé, 2001), which is roughly in the range of the present results (17–20 NH groups) and also agrees with literature reports of 18–19 free amino groups per mol BLG AB (Keppler et al., 2014; Rade-Kukic, Schmitt, & Rawel, 2011). Thus, no modifications on the lysine residues were found for the present recombinant BLG variants which was confirmed by the MS data (Table 1). A significantly higher number of amino groups would have indicated hydrolysis by *e.g.*, oxidation (Church, Swaisgood, Porter, & Catignani, 1983; Liu & Xiong, 2000) while a significantly lower number would indicate blocking or reduced accessibility of the amino group for the OPA reagent, as caused by *e.g.* lactozylation or aggregation (Kerkaert et al., 2011; Losito, Stringano, Carulli, & Palmisano, 2010; Norwood et al., 2016).

With respect to the amount of accessible thiol (SH) groups, there seem to be only minor structural differences. The presented results are comparable to the 0.2–0.3 mol SH groups per mol protein which have been reported for a correctly folded BLG AB in the native state (Kehoe et al., 2007; Kehoe, Remondetto, Subirade, Morris, & Brodkorb, 2008; Keppler et al., 2014), where the free thiol group of Cys121 is mostly inaccessible. A maximum of 1 mol SH group per mol protein can be measured when BLG would be completely unfolded. The significantly higher amount of accessible SH groups of rBLG B could indicate minor

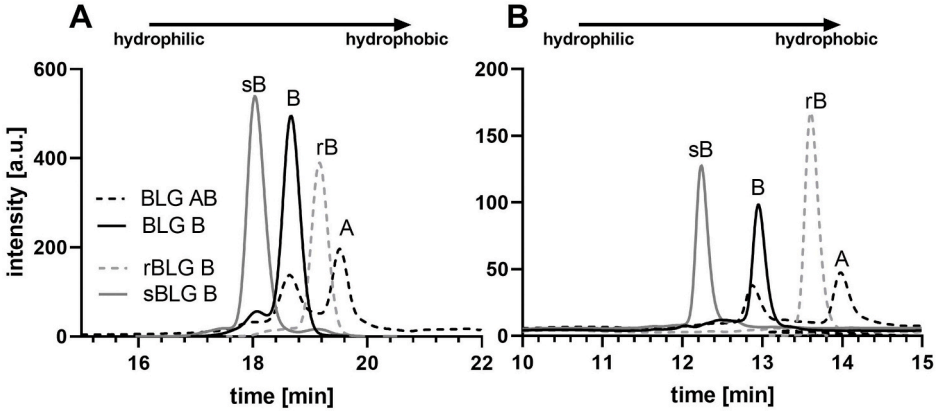

Fig. 4. Detail of RP-HPLC chromatograms of different BLG variants: **A)** Native monomers and **B)** unfolded monomers. The BLG AB reference (dotted black line) shows the presence of both isoforms A and B denoted as A and B in the chromatogram, sB and rB indicate recombinant variants sBLG B and rBLG B, respectively.

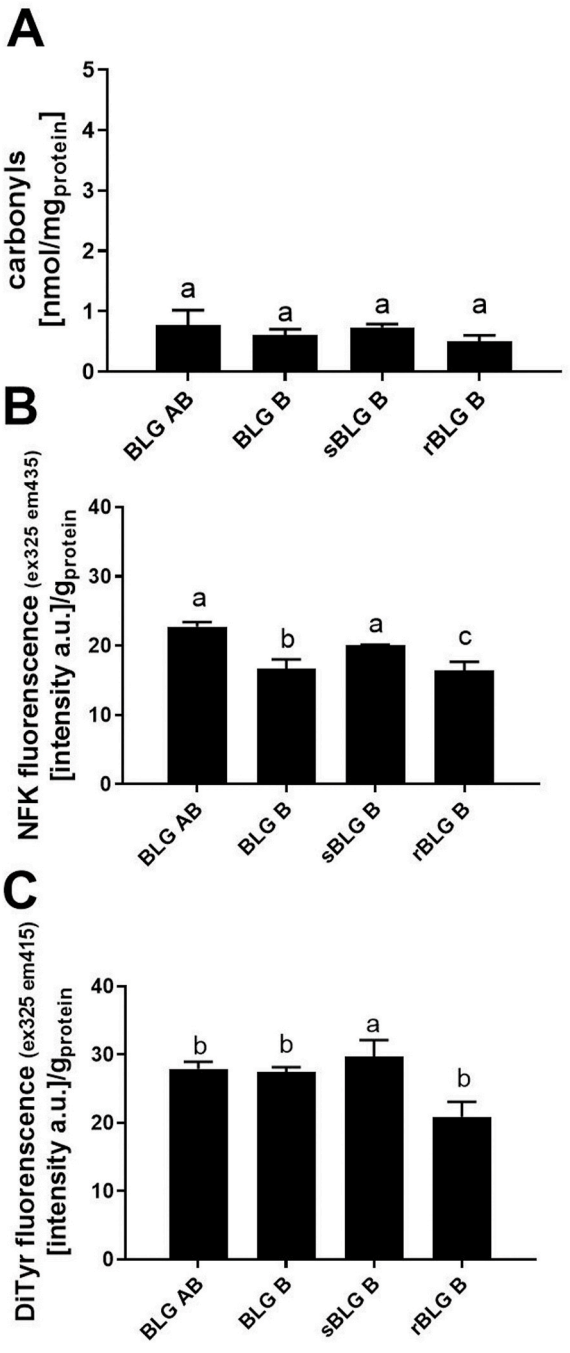

Fig. 5. Protein oxidation markers: A) protein-bound carbonyls, B) N-formylkynurenine (NFK) fluorescence and C) dityrosine (DiTyr) fluorescence) for different BLG variants. All measurements were conducted in triplicate and are listed as mean ± standard deviation. Different letters indicate statistically significant differences ($p < 0.05$).

folding differences, higher structural flexibility of the protein , or thiol-containing impurities. Since the FTIR results show no significant differences, the secondary structure seems to be mostly unaffected: The observed conformation of all BLG variants (Fig. 2A and B) is mostly comparable and in line with other FTIR analyses for native BLG B or BLG AB (Keppler et al., 2015; Panick et al., 1999). In addition, the Trp fluorescence analyses (Fig. 2C) also indicate no significant intensity increases or wavelength shifts which would have been indicative of conformational differences between the proteins for example with respect to solvent accessibility (Eftink & Ghiron, 1976; Heyn et al., 2019). The presented results confirm that both recombinant proteins are

Table 4
Adsorption parameters (*lag*-time, interfacial adsorption rate, and interfacial tension) for BLG AB, BLG B, rBLG B, and sBLG B.

	BLG AB	BLG B	rBLG B	sBLG B
lag-time [s]	27.9 ± 11.4[b]	12.3 ± 3.4[a,b]	6.8 ± 1.4[a]	9.8 ± 4.7[a]
Interfacial adsorption rate [mN $m^{-1}s^{-1}$]	−1.1 ± 0.7[b]	−0.1 ± 0.0[a]	−0.5 ± 0.3[a,b]	−0.9 ± 0.4[a,b]
Interfacial tension for t→∞ [mN m^{-1}]	15.8 ± 0.7[a]	20.2 ± 0.3[b]	14.9 ± 1.0[a]	16.7 ± 1.1[a]

[a] and [b]: significantly different values ($p < 0.05$) are indicated with small letters for a row.

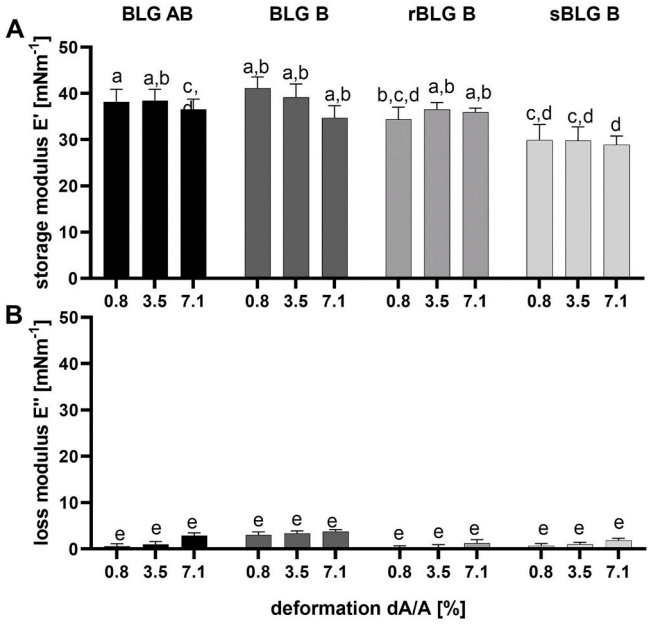

Fig. 6. A) Storage modulus E' and **B)** loss modulus E'' of the interfacial film of BLG AB, BLG B, rBLG B, and sBLG B at the deformation of the interfacial area of 0.8, 3.5 and 7.0%. Different letters (a–e) show significant differences between the values ($p < 0.05$).

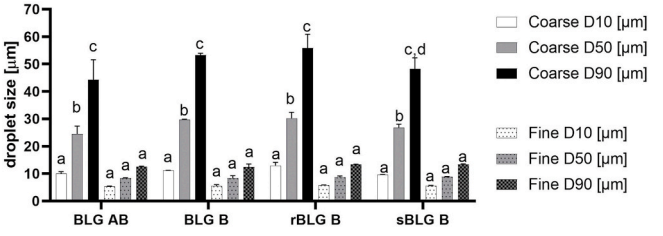

Fig. 7. Oil droplet size D10 (white), D50 (light grey), D90 (black) for the coarse (filled bars) and the fine emulsion (dotted bars) stabilized with BLG AB, BLG B, rBLG B or sBLG B derived by premix membrane emulsification. Different letters (a–d) show significant differences between the values ($p < 0.05$).

indeed correctly folded, as stated previously by Loch et al. (2016) (Table 1, Fig. 1). In addition, all samples showed an overall low oxidation with respect to protein carbonyl (<1 nmol/mg protein) or fluorescence formation (<30 Int A.U.) (Fig. 5). Similar low values were found for whey protein powders (Keppler, Heyn, Meissner, Schrader, & Schwarz, 2019; Scheidegger et al., 2010; Semagoto et al., 2014).

Hence, the presented results confirm that the recombinant production in the bacterial host *E. coli* and isolation procedure have no detrimental effect on the nativity, PTMs, and oxidative state of the produced BLG variants.

Overall, the MD simulations confirm that the BLG variants showed high structural similarities (Table 1), with sBLG B performing most similar to the commercial BLG B, while rBLG B exhibits slightly reduced structure stability as indicated by the significantly higher root mean squared deviation (0.36 nm vs. 0.29 nm), the higher radius of gyration (1.54 nm vs. 1.52 nm) and the higher solvent accessibility (183 nm^2 vs. 178 nm^2).

The determination of the quaternary structure of the BLG variants by AUC as well as by DLS also confirms a similar monomer/dimer behavior for the recombinant variants as well as similar K_D for BLG AB and recombinant BLG Bs (Fig. 3A and B, Table 2). Correspondingly, MD simulations at neutral pH resulted in the same monomer/monomer binding energy for all variants. The results are in agreement with the literature on the monomer/dimer behavior of BLG B and rBLG B (Mercadante et al., 2012; Kristiansen, Otte, Ipsen, & Qvist, 1998). BLG was found to be predominantly monomeric near pH 2 and 9, while the dimer form prevails at pH 7 (Renard, Lefebvre, Griffin, & Griffin, 1998; Verheul, Pedersen, Roefs, & Kruif, 1999).

4.2. Physicochemical properties

So far, the results confirmed that neither the protein production system nor the isolation process affects the protein's structural properties (i.e., high purity, native conformation (Fig. 2), neither oxidative (Fig. 5) nor glycozylation based PTM (Table 1)). In addition, all BLG variants showed similar folding and similar monomer/dimer equilibrium (Figs. 1, Figure 2, and Fig. 3, Table 2). Now, denaturation temperature at pH 7, isoelectric point, zeta potential at pH 7, acid solubility, and hydrophobicity were analyzed and compared (Tables 1–3).

As a first observation, the rBLG B displayed incomplete resolubilization after lyophilization resulting in some undissolved protein aggregates (<7%) which was not observed for the other variants. The aggregates were removed by centrifugation or filtration (0.45 μm membrane) to allow spectroscopic or scattering analyses (e.g., protein oxidation, OPA, RSH, DLS, AUC). The reason for the limited resolubilization, which only concerns rBLG B, is unclear.

A significant difference can be observed for both recombinant variants compared to the other BLG variants with respect to the thermal stability (Table 3). While BLG B and BLG AB exhibit denaturation temperatures of approximately 77 °C in water (pH 7), sBLG B denatures at ~78 °C, and rBLG B at ~80 °C. In other studies, denaturation temperatures of BLG AB determined at neutral pH and low ionic strength varied between 69.2 and 80.1 °C (Tolkach & Kulozik, 2007; Busti, Gatti, & Delorenzi, 2005). The results of the present study are consistent with the reported denaturation temperature range. The reported bandwidth of variation (10 K) of these measurements are caused by differences in protein purity or analysis methodology. In contrast to the present finding, CD analyses gave evidence of a slightly lower thermal stability for sBLG B than BLG B (Loch et al., 2016). Also these differences could be caused by using different purification strategies of sBLG B, different analysis methods and conditions (e.g. protein concentration, salt concentrations). Nevertheless, an effect of the modified N-terminus on the denaturation temperature cannot be excluded, since a modified N-terminus can have a stabilizing or even destabilizing effect on other proteins (Chaudhuri, Horii, & Yoda, 1999) Schultz et al., 1992). However, also the native genetic variants BLG A, B, and C (which differ by 1 or 2 amino acids) are found to diverge in their T_d each by 5 K in phosphate buffer (pH 7) (Keppler, Sönnichsen, Lorenzen, & Schwarz, 2014) or other solvents (Imafidon, Ng-Kwai-Hang, Harwalkar, & Ma, 1991; McLean, Graham, Ponzoni, & McKenzie, 1987). Thus, the observed deviations of the recombinant proteins are within the natural variances of BLG.

In general, an IEP of 5.1–5.2 is reported for BLG in the literature (Yan et al., 2013) which is roughly in the range of our samples (IEP 4.9–5.4). However, the IEP of commercial BLG B sample with 4.7 is lower than expected (*i.e.*, 5.23 for native BLG B). This deviation could indicate denaturation, but this was not observed in FTIR and Trp fluorescence (Fig. 2). In addition, the different IEP of the commercial BLG B was also not reflected in the results of the quarternary structure analyses by AUC (Fig. 3) or DLS (Table 2). Low ionic strength can lead to a loss of solubility of globular proteins and the presence of multivalent (bound) anions can extend the iso-ionic range to a pH of 4.6. Different ions or ion concentrations in the commercial BLG B sample (obtained from Sigma Aldrich) compared to those that have been isolated and dialyzed by our groups (BLG AB, sBLG B, and rBLG B) could be an explanation for this (de Wit & Kessel, 1996). Because of the high similarity of the IEP of the other BLG variants, the acid solubility (*i.e.*, solubility at pH 4.6) can still be used as a measure of protein nativity in these cases. This analysis is strongly dependent on the IEP shift between native and denatured BLG (Table 1), thus denatured BLG precipitates at pH 4.6 while the native protein remains in solution (Pizzano, Manzo, Nicolai, & Addeo, 2012; Toro-Sierra et al., 2013). For the BLG AB and recombinant B variants, the high acid solubility can be translated to a high nativity, which is also in line with FTIR (Fig. 2A), Trp fluorescence (Fig. 2C) and the number of accessible SH groups (Table 1). As expected, the low IEP observed in BLG B also correlates with a reduced acid solubility of 88% and it can be hypothesized that this result is likely rather connected to the solubility issues discussed before and not to its state of denaturation because FTIR and Trp fluorescence indicate high nativity.

Finally, the protein hydrophobicity was analyzed using an RP-HPLC, which is independent of the ionic strength in the samples. The observed difference in elution time indicates that BLG A is more hydrophobic than BLG B which has already been reported by Keppler et al. (2017) or Ruprichova et al. (2014) using a similar chromatographic separation technique. Although, at neutral pH values, the overall net negative charge for BLG A is higher than BLG B because of the negative charge of the Asp at position 64 (Keppler, Sönnichsen et al., 2014). Overall it is difficult to forecast the hydrophobic behavior of proteins in chromatographic separations based only on the amino acid sequence (Mahn, Lienqueo, & Asenjo, 2004). It was shown, that the retention in RP-HPLC that is based on hydrophobic interactions is strongly influenced by the flexibility of proteins (To & Lenhoff, 2007). This explains the observed behavior of BLG A and BLG B in RP-HPLC: BLG A interacts more strongly with the chromatographic stationary phase than BLG B despite only two changes in the amino acid composition (BLG A: Asp64, Ala118. BLG B: Gly64, Val118). Based on the change in Position 118, which is located inside the protein's core, Qin et al. reported a higher flexibility for BLG A (Qin, Bewley, Creamer, Baker, & Jameson, 1999) that may explain the observed behavior of BLG variants A and B in RP-HPLC. A simpler relationship between amino acid exchange and hydrophobicity can be seen in the recombinant variants, probably because the N-terminal amino acid exchange has less effect on the protein backbone flexibility than a mutation in the core of the protein. The substitution of the more polar Ser in sBLG B against the nonpolar Ile explains the lower hydrophobicity of sBLG B compared to BLG B. The rBLG B, on the other hand, contains an additional nonpolar Met, which shifts the protein to a higher residence time in RP-HPLC. However, further investigation on protein structure and on the flexibility of the variants sBLG B and rBLG B is necessary to explain the elution order.

4.3. Emulsifying properties

The present results show that the recombinant variants are structurally very similar. The main differences between rBLG B and the other BLG variants are the denaturation temperature and the resolubilization behavior. Therefore, the impact on the functional level (*i.e.*, interfacial behavior and emulsifying properties) was investigated in the following.

The migration-driven interfacial activity of all BLG variants was compared using pendant drop analysis. The dynamic interfacial tension shows that the *lag*-time and equilibrium interfacial tension (Table 4) are roughly in the range reported previously for whey protein isolate rich in BLG in water (pH 7), adsorbed at a rapeseed O/W interface (Keppler

et al., 2018; Böttcher, Keppler, & Drusch, 2017). Deviations are likely caused by different methodologies and purities between the different studies (BLG vs. whey protein isolate, different oil phases, and different ions) (Beverung, Radke, & Blanch, 1999; Geerts, Nikiforidis, van der Goot, & van der Padt; Keppler et al., 2018; Mackie, Husband, Holt, & Wilde, 1999; Tenorio, Jong, Nikiforidis, Boom, & van der Goot, 2017).

All three measured surface properties (*lag*-time, adsorption rate and equilibrium interfacial tension) are the result of different, complexly interacting protein properties, so they can rarely be traced back to a single effect and further analyses are needed to elucidate this. In the following, the individual properties of the interfacial activity are discussed in more detail.

The *lag*-time correlates with the initial protein adsorption (short-term effects). It is characterized by protein migration through the bulk phase. In addition, the *lag*-time ends as soon as a protein adsorbs and unfolds at an interface, thus a high interface denaturation kinetics of the protein and a low surface charge correlate with a reduced *lag*-time (Beverung et al., 1999; Keppler et al., 2018). The *lag*-times were similar with approximately 10 s for all variants except for the BLG AB mixture with 28 s. The similar *lag*-time for all BLG B variants can be explained by their similar size (i.e., similar migration speed) and similar zeta-potential (Table 2). The higher thermal stability of the recombinant variants (Table 3) seems to have no overall impact on the *lag*-time. The higher *lag*-time of the BLG AB might be explained by the higher net negative surface charge of the BLG A at pH 7, causing less attraction to hydrophobic interfaces than observed for BLG B. Although the overall hydrophobicity of BLG A in HPLC is highest (Fig. 4, see discussion above), the single negative charge on its surface can reduce the initial adsorption compared to BLG B (Mackie et al., 1999).

The adsorption rate (Table 4) correlates to the mid-term structural rearrangement of the protein at the interface. The overall hydrophobicity of the protein, molecular flexibility and conformational stability were found to be of importance (Beverung et al., 1999; Keppler et al., 2018). Again, all BLG B variants showed similar adsorption rates, while the BLG AB differed. The high molecular flexibility of BLG A could be an explanation for the overall faster unfolding and rearrangement of BLG AB, despite its single negative charge on the surface. However, sBLG B also showed a fast surface adsorption rate, but there was no evidence of a high structural flexibility and/or a low overall hydrophobicity as it showed the lowest stationary phase binding in HPLC (Fig. 4). Differences in the adsorption rate can also be due to different electrostatic interactions and densities of the BLG AB dimer compared to the BLG B homodimers at pH 7 (Schestkowa et al., 2019).

The equilibrium interfacial tension correlates to the long-term effects, such as overall protein packing density at the interface, interface rearrangement and network formation. The equilibrium interfacial tension was significantly lower for BLG B compared to all other variants. This could be due to a lower packing density of BLG B at the interface (Keppler et al., 2018; Schestkowa et al., 2019), although the high elastic properties of the BLG B surface film indicates a densely packed interface or a well interconnected film (Fig. 6).

All BLG films at the O/W interface exhibited viscoelastic properties (E' > E") with the sBLG B film showing less elastic properties in the film compared to the commercial BLG B. This can indicate a less densely packed interface (Bos & van Vliet, 2001; Engelhardt et al., 2013; Keppler et al., 2017; Sagis & Scholten, 2014) and a lower mechanical stability, but on the other hand, the recombinant variants showed no shear dependent loss of storage modulus which confirms the stability against some mechanical stress (Fig. 6).

Finally, all BLG variants resulted in emulsions with similar oil droplet size distribution and creaming stability (Fig. 7). The droplet size of the coarse emulsion stabilized with BLG AB (D50 = 25 μm) was comparable to BLG B stabilized water/MCT-oil emulsions prepared with a high-pressure homogenizer (10–20 μm) (Böttcher et al., 2017). The observed faster adsorption kinetics of the recombinant BLG variants (Fig. 4) probably does not take effect in the investigated time range of the emulsification process. The emulsion creaming stability is likewise not different for the different proteins, probably due to the fact that the low interfacial elasticity of the recombinant variants is compensated by the high protein concentration (saturated interface) and will rather be observable in less concentrated samples. Other homogenization processes (*e.g.*, ultrasonic), other continuous phases as well as other protein concentrations could lead to differences in the adsorption behavior, achieved droplet size and then displaying the observed differences in adsorption behavior and interfacial stability.

In conclusion, in the present study similar emulsion properties were found for all recombinant BLG variants as well as for bovine BLG isolated from milk.

5. Conclusion

The presented preparation and isolation of recombinant BLG B variants resulted in proteins with high nativity, purity, and no significant PTM.

Based on the simulations and measurements shown, the sBLG B seemed to exhibit higher equivalence with commercial bovine BLG B, while the elongated N-terminal of the rBLG B led to deviations in radius and structural stability. Nevertheless, all variants are structurally very similar. Consequently, the emulsification properties are not affected by the structural differences of the recombinant variants. Thus, these proteins can be used from a functional point of view as bovine whey protein substitutes with regard to emulsion production. As scientific/research perspective, these recombinant proteins can be used as starting base for targeted modifications of BLG for applications in food technology beyond the varieties produced in this study.

Further tests regarding other homogenization methods, but also other process steps such as foaming, drying, and gelling behavior are still required in order to obtain a more holistic view of the performance and the substantial equivalence of these proteins. These investigations are relevant to assess the commercial and environmental sustainability of this alternative concept of producing proteins.

Declaration of competing interest

None.

CRediT authorship contribution statement

Julia K. Keppler: Project administration, Funding acquisition, Conceptualization, Resources, Writing - original draft, Visualization, Supervision. **Anja Heyse:** Conceptualization, Investigation, Formal analysis, Writing - original draft. **Eva Scheidler:** Investigation, Formal analysis, Writing - original draft. **Maximilian J. Uttinger:** Investigation, Formal analysis, Writing - original draft. **Laura Fitzner:** Investigation, Formal analysis, Writing - original draft. **Uwe Jandt:** Formal analysis, Writing - original draft, Funding acquisition. **Timon R. Heyn:** Investigation, Formal analysis, Writing - original draft. **Vanessa Lautenbach:** Investigation, Formal analysis, Writing - original draft. **Joanna I. Loch:** Writing - review & editing, Visualization, Resources. **Jonas Lohr:** Investigation, Writing - original draft. **Helena Kieserling:** Writing - review & editing, Visualization. **Gabriele Günther:** Investigation. **Elena Kempf:** Investigation. **Jan-Hendrik Grosch:** Investigation. **Krzysztof Lewiński:** Writing - review & editing, Resources. **Dieter Jahn:** Writing - review & editing, Resources, Funding acquisition, Supervision. **Christian Lübbert:** Investigation, Writing - original draft. **Wolfgang Peukert:** Funding acquisition, Writing - review & editing, Supervision, Resources. **Ulrich Kulozik:** Funding acquisition, Writing - review & editing, Supervision, Resources. **Stephan Drusch:** Funding acquisition, Writing - review & editing, Supervision, Resources. **Rainer Krull:** Funding acquisition, Conceptualization, Writing - review & editing, Supervision, Resources. **Karin Schwarz:** Funding acquisition, Conceptualization, Writing - review & editing, Supervision, Resources.

Rebekka Biedendieck: Project administration, Funding acquisition, Conceptualization, Resources, Writing - original draft, Supervision.

Acknowledgments

The authors gratefully acknowledge the financial support provided by the German Research Foundation (DFG) within the priority program, SPP1934 "*DiSPBiotech – Dispersity, structural and phase modifications of proteins and biological agglomerates in biotechnological processes*". TU Braunschweig would like to thank Beate Jaschok-Kentner, Helmholtz Centre for Infection Research, Department of Molecular Structural Biology, Braunschweig, Germany, for N-terminal protein sequencing. Kiel University acknowledges the skillful help of Jesco Reimers, Division of Food Technology, Kiel University, Germany, with protein fluorescence measurements. ES and UK acknowledge the professional technical work of Claudia Hengst in conducting the HPLC analysis. UJ acknowledges partial funding by BMBF (grant 031B0222).

Appendix A. Supplementary data

Supplementary data to this article can be found online at https://doi.org/10.1016/j.foodhyd.2020.106132.

References

Batt, C. A., Rabson, L. D., Wong, D. W., & Kinsella, J. E. (1990). Expression of recombinant bovine beta-lactoglobulin in *Escherichia coli*. *Agricultural & Biological Chemistry, 54*(4), 949–955.

Beverung, C. J., Radke, C. J., & Blanch, H. W. (1999). Protein adsorption at the oil/water interface: Characterization of adsorption kinetics by dynamic interfacial tension measurements. *Biophysical Chemistry, 81*(1), 59–80.

Bhat, Z. F., Kumar, S., & Fayaz, H. (2015). *In vitro* meat production: Challenges and benefits over conventional meat production. *Journal of Integrative Agriculture, 14*(2), 241–248.

Bos, M. A., & van Vliet, T. (2001). Interfacial rheological properties of adsorbed protein layers and surfactants: A review. *Advances in Colloid and Interface Science, 91*(3), 437–471.

Böttcher, S., Keppler, J. K., & Drusch, S. (2017). Mixtures of *Quillaja saponin* and beta-lactoglobulin at the oil/water-interface: Adsorption, interfacial rheology and emulsion properties. *Colloids and Surfaces A: Physicochemical and Engineering Aspects, 518*, 46–56.

Brown, P. H., & Schuck, P. (2006). Macromolecular size-and-shape distributions by sedimentation velocity analytical ultracentrifugation. *Biophysical Journal, 90*(12), 4651–4661.

Busti, P., Gatti, C. A., & Delorenzi, N. J. (2005). Thermal unfolding of bovine β-lactoglobulin studied by UV spectroscopy and fluorescence quenching. *Food Research International, 38*(5), 543–550.

Chaudhuri, TK, Horii, K, Yoda, T, et al. (1999). Effect of the extra n-terminal methionine residue on the stability and folding of recombinant alpha-lactalbumin expressed in Escherichia coli. *Journal of Molecular Biology, 285*(3), 1179–1194. https://doi.org/10.1006/jmbi.1998.2362.

Chevalier, F., Chobert, J.-M., Popineau, Y., Nicolas, M. G., & Haertlé, T. (2001). Improvement of functional properties of β-lactoglobulin glycated through the Maillard reaction is related to the nature of the sugar. *International Dairy Journal, 11*(3), 145–152.

Cho, Y., Gu, W., Watkins, S., Lee, S. P., Kim, T. R., Brady, J. W., et al. (1994). Thermostable variants of bovine beta-lactoglobulin. *Protein Engineering, 7*(2), 263–270.

Church, F. C., Swaisgood, H. E., Porter, D. H., & Catignani, G. L. (1983). Spectrophotometric assay using o-phthaldialdehyde for determination of proteolysis in milk and isolated milk Proteins. *Journal of Dairy Science, 66*(6), 1219–1227.

Dekkers, B. L., Boom, R. M., & van der Goot, A. J. (2018). Structuring processes for meat analogues. *Trends in Food Science & Technology, 81*, 25–36.

Denton, H., Smith, M., Husi, H., Uhrin, D., Barlow, P. N., Batt, C. A., et al. (1998). Isotopically labeled bovine β-lactoglobulin for NMR studies expressed in *Pichia pastoris*. *Protein Expression and Purification, 14*(1), 97–103.

de Wit, J. N., & Kessel, T.v. (1996). Effects of ionic strength on the solubility of whey protein products. A colloid chemical approach. *Food Hydrocolloids, 10*(2), 143–149.

Dombrowski, J., Gschwendtner, M., Saalfeld, D., & Kulozik, U. (2018). Salt-dependent interaction behavior of β-Lactoglobulin molecules in relation to their surface and foaming properties. *Colloids and Surfaces A: Physicochemical and Engineering Aspects, 558*, 455–462.

Dumpler, J., Wohlschläger, H., & Kulozik, U. (2017). Dissociation and coagulation of caseins and whey proteins in concentrated skim milk heated by direct steam injection. *Dairy Science & Technology, 96*(6), 807–826.

Edman, P., & Begg, G. (1967). A protein sequenator. In C. Liébecq (Ed.), *European journal of biochemistry* (pp. 80–91). Berlin, Heidelberg: Springer Berlin Heidelberg.

Eftink, M. R., & Ghiron, C. A. (1976). Exposure of tryptophanyl residues in proteins. Quantitative determination by fluorescence quenching studies. *Biochemistry, 15*(3), 672–680.

Ellman, G. L. (1959). Tissue sulfhydryl groups. *Archives of Biochemistry and Biophysics, 82*(1), 70–77.

Engelhardt, K., Lexis, M., Gochev, G., Konnerth, C., Miller, R., Willenbacher, N., et al. (2013). pH effects on the molecular structure of β-lactoglobulin modified air–water interfaces and its impact on foam rheology. *Langmuir, 29*(37), 11646–11655.

Geerts, M. E. J., Nikiforidis, C. V., van der Goot, A. J., & van der Padt, A. Protein nativity explains emulsifying properties of aqueous extracted protein components from yellow pea. Food Structure 14, 104-111.

Heyn, T. R., Garamus, V. M., Neumann, H. R., Uttinger, M. J., Guckeisen, T., Heuer, M., et al. (2019). Influence of the polydispersity of pH 2 and pH 3.5 beta-lactoglobulin amyloid fibril solutions on analytical methods. *European Polymer Journal, 120*, 109211.

Hundschell, C. S., Bäther, S., Drusch, S., & Wagemans, A. M. (2020). Osmometric and viscometric study of levan, β-lactoglobulin and their mixtures. *Food Hydrocolloids, 101*, 105580.

Imafidon, G. I., Ng-Kwai-Hang, K. F., Harwalkar, V. R., & Ma, C.-Y. (1991). Differential scanning calorimetric study of different genetic variants of β-lactoglobulin. *Journal of Dairy Science, 74*(8), 2416–2422.

Jayat, D., Gaudin, J.-C., Chobert, J.-M., Burova, T. V., Holt, C., McNae, I., et al. (2004). A recombinant C121S mutant of bovine β-lactoglobulin is more susceptible to peptic digestion and to denaturation by reducing agents and heating. *Biochemistry, 43*(20), 6312–6321.

Kaminski, G. A., Friesner, R. A., Tirado-Rives, J., & Jorgensen, W. L. (2001). Evaluation and reparametrization of the OPLS-AA force field for proteins via comparison with accurate quantum chemical calculations on peptides. *The Journal of Physical Chemistry B, 105*(28), 6474–6487.

Kayser, J. J., Arnold, P., Steffen-Heins, A., Schwarz, K., & Keppler, J. K. (2020). Functional ethanol-induced fibrils: Influence of solvents and temperature on amyloid-like aggregation of beta-lactoglobulin. *Journal of Food Engineering, 270*, 109764.

Kehoe, J. J., Brodkorb, A., Mollé, D., Yokoyama, E., Famelart, M.-H., Bouhallab, S., et al. (2007). Determination of exposed sulfhydryl groups in heated b-lactoglobulin A using IAEDANS and mass spectrometry. *Journal of Agricultural and Food Chemistry, 55*(17), 7107–7113.

Kehoe, J. J., Remondetto, G. E., Subirade, M., Morris, E. R., & Brodkorb, A. (2008). Tryptophan-mediated denaturation of β-lactoglobulin A by UV irradiation. *Journal of Agricultural and Food Chemistry, 56*(12), 4720–4725.

Keppler, J. K., Koudelka, T., Palani, K., Stuhldreier, M. C., Temps, F., Tholey, A., et al. (2014a). Characterization of the covalent binding of allyl isothiocyanate to β-lactoglobulin by fluorescence quenching, equilibrium measurement, and mass spectrometry. *Journal of Biomolecular Structure & Dynamics, 32*(7), 1103–1117.

Keppler, J., Martin, D., Garamus, V., Berton-Carabin, C., Nipoti, E., Coenye, T., et al. (2017). Functionality of whey proteins covalently modified by allyl isothiocyanate. Part 1 physicochemical and antibacterial properties of native and modified whey proteins at pH 2 to 7. *Food Hydrocolloids, 65*, 130–143.

Keppler, J. K., Martin, D., Garamus, V. M., & Schwarz, K. (2015). Differences in binding behavior of (-)-epigallocatechin gallate to beta-lactoglobulin heterodimers (AB) compared to homodimers (A) and (B). *Journal of Molecular Recognition, 28*(11), 656–666.

Keppler, Heyn, Meissner, Schrader, & Schwarz. (2019). Protein oxidation during temperature-induced amyloid aggregation of beta-lactoglobulin. *Food Chemistry, 289*, 223–231.

Keppler, J. K., Sönnichsen, F. D., Lorenzen, P.-C., & Schwarz, K. (2014b). Differences in heat stability and ligand binding among β-lactoglobulin genetic variants A, B and C using 1H NMR and fluorescence quenching. *Biochimica et Biophysica Acta (BBA) - Proteins & Proteomics, 1844*(6), 1083–1093.

Keppler, J. K., Steffen-Heins, A., Berton-Carabin, C. C., Ropers, M.-H., & Schwarz, K. (2018). Functionality of whey proteins covalently modified by allyl isothiocyanate. Part 2: Influence of the protein modification on the surface activity in an O/W system. *Food Hydrocolloids, 81*, 286–299.

Kerkaert, B., Mestdagh, F., Cucu, T., Aedo, P. R., Ling, S. Y., & De Meulenaer, B. (2011). Hypochlorous and peracetic acid induced oxidation of dairy proteins. *Journal of Agricultural and Food Chemistry, 59*(3), 907–914.

Kim, T. R., Goto, Y., Hirota, N., Kuwata, K., Denton, H., Wu, S. Y., et al. (1997). High-level expression of bovine beta-lactoglobulin in *Pichia pastoris* and characterization of its physical properties. *Protein Engineering, 10*(11), 1339–1345.

Kristiansen, K. R., Otte, J., Ipsen, R., & Qvist, K. B. (1998). Large-scale preparation of β-lactoglobulin A and B by ultrafiltration and ion-exchange chromatography. *International Dairy Journal, 8*(2), 113–118.

Lam, R. S. H., & Nickerson, M. T. (2014). The effect of pH and heat pre-treatments on the physicochemical and emulsifying properties of β-lactoglobulin. *Food Biophysics, 9*(1), 20–28.

Levine, R. L., Garland, D., Oliver, C. N., Amici, A., Climent, I., Lenz, A. G., et al. (1990). Determination of carbonyl content in oxidatively modified proteins. *Methods in Enzymology, 186*, 464–478.

Liu, G., & Xiong, Y. L. (2000). Oxidatively induced chemical changes and interactions of mixed myosin, β-lactoglobulin and soy 7S globulin. *Journal of the Science of Food and Agriculture, 80*(11), 1601–1607.

Loch, J. I., Bonarek, P., Tworzydlo, M., Polit, A., Hawro, B., Lach, A., et al. (2016). Engineered beta-lactoglobulin produced in *E. coli*: Purification, biophysical and structural characterisation. *Molecular Biotechnology, 58*(10), 605–618.

Losito, I., Stringano, E., Carulli, S., & Palmisano, F. (2010). Correlation between lactosylation and denaturation of major whey proteins: An investigation by liquid

chromatography-electrospray ionization mass spectrometry. *Analytical and Bioanalytical Chemistry, 396*(6), 2293–2306.
Mackie, A. R., Husband, F. A., Holt, C., & Wilde, P. J. (1999). Adsorption of β-Lactoglobulin variants A and B to the air–water interface. *International Journal of Food Science and Technology, 34*(5-6), 509–516.
Mahn, A, Lienqueo, ME, & Asenjo, JA (2004). Effect of surface hydrophobicity distribution on retention of ribonucleases in hydrophobic interaction chromatography. *Chromatogr A, 1043*(1), 47–55. https://doi.org/10.1016/j.chroma.2004.03.021.
Marti-Renom, M. A., Stuart, A. C., Fiser, A., Sanchez, R., Melo, F., & Sali, A. (2000). Comparative protein structure modeling of genes and genomes. *Annual Review of Biophysics and Biomolecular Structure, 29*, 291–325.
McLean, D. M., Graham, E. R. B., Ponzoni, R. W., & McKenzie, H. A. (1987). Effects of milk protein genetic variants and composition on heat stability of milk. *Journal of Dairy Research, 54*(2), 219–235.
Mercadante, D., Melton, L. D., Norris, G. E., Loo, T. S., Williams, M. A. K., Dobson, R. C. J., et al. (2012). Bovine b-lactoglobulin is dimeric under imitative physiological conditions: Dissociation equilibrium and rate constants over the pH range of 2.5–7.5. *Biophysical Journal, 103*, 303–312.
Mishyna, M., Chen, J., & Benjamin, O. (2020). Sensory attributes of edible insects and insect-based foods – future outlooks for enhancing consumer appeal. *Trends in Food Science & Technology, 95*, 141–148.
Norwood, E.-A., Chevallier, M., Le Floch-Fouéré, C., Schuck, P., Jeantet, R., & Croguennec, T. (2016). Heat-induced aggregation properties of whey proteins as affected by storage conditions of whey protein isolate powders. *Food and Bioprocess Technology, 9*(6), 993–1001.
Panick, G., Malessa, R., & Winter, R. (1999). Differences between the pressure- and temperature-induced denaturation and aggregation of beta-lactoglobulin A, B, and AB monitored by FT-IR spectroscopy and small-angle X-ray scattering. *Biochemistry, 38*(20), 6512–6519.
Paul, A. A., Kumar, S., Kumar, V., & Sharma, R. (2019). Milk Analog: Plant based alternatives to conventional milk, production, potential and health concerns. *Critical Reviews in Food Science and Nutrition*, 1–19.
Pizzano, R., Manzo, C., Nicolai, M. A., & Addeo, F. (2012). Occurrence of major whey proteins in the pH 4.6 insoluble protein fraction from UHT-treated milk. *Journal of Agricultural and Food Chemistry, 60*(32), 8044–8050.
Ponniah, K., Loo, T. S., Edwards, P. J. B., Pascal, S. M., Jameson, G. B., & Norris, G. E. (2010). The production of soluble and correctly folded recombinant bovine β-lactoglobulin variants A and B in *Escherichia coli* for NMR studies. *Protein Expression and Purification, 70*(2), 283–289.
Qin, Bin, Y., Bewley, Maria, C., Creamer, Lawrence, K., Baker, Edward, N., & Jameson, Geoffrey, B. (1999). Functional Implications of Structural Differences Between Variants A and B of Bovine Beta-Lactoglobulin. *Protein Science, 8*(1), 75–83.
Rade-Kukic, K., Schmitt, C., & Rawel, H. M. (2011). Formation of conjugates between β-lactoglobulin and allyl isothiocyanate: Effect on protein heat aggregation, foaming and emulsifying properties. *Food Hydrocolloids, 25*(4), 694–706.
Renard, D., Lefebvre, J., Griffin, M. C. A., & Griffin, W. G. (1998). Effects of pH and salt environment on the association of [beta]-lactoglobulin revealed by intrinsic fluorescence studies. *International Journal of Biological Macromolecules, 22*(1), 41–49.
Righetti, P., Gianazza, E., Gelfi, C., & Chairi, M. (1990). *Gel electrophoresis of proteins: A practical approach* (2nd ed.). Oxford: Oxford University Press.
Roth, M. (1971). Fluorescence reaction for amino acids. *Analytical Chemistry, 43*(7), 880–882.
Ruprichová, L., Králová, M., Borkovcová, I., Vorlová, L., & Bedáňová, I. (2014). Determination of whey proteins in different types of milk. *Acta Veterinaria Brno, 83*(1), 67–72.
Sagis, L. M. C., & Scholten, E. (2014). Complex interfaces in food: Structure and mechanical properties. *Trends in Food Science & Technology, 37*(1), 59–71.
Scheidegger, D., Pecora, R. P., Radici, P. M., & Kivatinitz, S. C. (2010). Protein oxidative changes in whole and skim milk after ultraviolet or fluorescent light exposure. *Journal of Dairy Science, 93*(11), 5101–5109.
Schestkowa, H., Wollborn, T., Westphal, A., Wagemans, A., Fritsching, U., & Drusch, S. (2019). Conformational state and charge determine the interfacial stabilization process of beta-lactoglobulin at preoccupied interfaces. *Journal of Colloid and Interface Science, 536*, 300–309.
Schultz, D. A., & Baldwin, R. L. (1992). Cis proline mutants of ribonuclease A. I. thermal stability. *Protein Science, 1*(7), 831–958.
Semagoto, H. M., Liu, D., Koboyatau, K., Hu, J., Lu, N., Liu, X., et al. (2014). Effects of UV induced photo-oxidation on the physicochemical properties of milk protein concentrate. *Food Research International, 62*, 580–588.
Sethi, S., Tyagi, S. K., & Anurag, R. K. (2016). Plant-based milk alternatives an emerging segment of functional beverages: A review. *Journal of Food Science & Technology, 53*(9), 3408–3423.
Stafford, W. F., & Sherwood, P. J. (2004). Analysis of heterologous interacting systems by sedimentation velocity: Curve fitting algorithms for estimation of sedimentation coefficients, equilibrium and kinetic constants. *Biophysical Chemistry, 108*(1), 231–243.
Tagliavia, M., & Nicosia, A. (2019). Advanced strategies for food-grade protein production: A new E. coli/lactic acid bacteria shuttle vector for improved cloning and food-grade expression. *Microorganisms, 7*(5), 116.
Tamm, F., & Drusch, S. (2017). Impact of enzymatic hydrolysis on the interfacial rheology of whey protein/pectin interfacial layers at the oil/water-interface. *Food Hydrocolloids, 63*, 8–18.
Tenorio, A. T., Jong, E. W. M.d., Nikiforidis, C. V., Boom, R. M., & van der Goot, A. J. (2017). Interfacial properties and emulsification performance of thylakoid membrane fragments. *Soft Matter, 13*(3), 608–618.
To, BC, & Lenhoff, AM (2007). Hydrophobic interaction chromatography of proteins. I. The effects of protein and adsorbent properties on retention and recovery. *J Chromatogr A., 1141*(2), 191–205. https://doi.org/10.1016/j.chroma.2006.12.020.
Tolkach, A., & Kulozik, U. (2007). Reaction kinetic pathway of reversible and irreversible thermal denaturation of beta-lactoglobulin. *Le Lait, 87*(4-5), 301–315.
Toro-Sierra, J., Tolkach, A., & Kulozik, U. (2013). Fractionation of α-lactalbumin and β-lactoglobulin from whey protein isolate using selective thermal aggregation, an optimized membrane separation procedure and resolubilization techniques at pilot plant scale. *Food and Bioprocess Technology, 6*(4), 1032–1043.
Ui, N. (1971). Isoelectric points and conformation of proteins I. Effect of urea on the behavior of some proteins in isoelectric focusing. *Biochimica et biophysics acta, 229*, 567–581.
US9924728B2, Patent, Pandya, R., Gandhi, P., Ji, S., Beauchamp, D., & Horn, L. (2018). *Food compositions comprising one or both of recombinant beta-lactoglobulin protein and recombinant alpha-lactalbumin protein*.
Uttinger, M. J., Heyn, T. R., Jandt, U., Wawra, S. E., Winzer, B., Keppler, J. K., et al. (2020). Measurement of length distribution of beta-lactoglobulin fibrils by multiwavelength analytical ultracentrifugation. *European Biophysics Journal* (in press).
Uttinger, M. J., Wawra, S. E., Guckeisen, T., Walter, J., Bear, A., Thajudeen, T., et al. (2019). A comprehensive Brownian dynamics approach for the determination of non-ideality parameters from analytical ultracentrifugation. *Langmuir, 35*(35), 11491–11502.
Van Der Spoel, D., Lindahl, E., Hess, B., Groenhof, G., Mark, A. E., & Berendsen, H. J. C. (2005). GROMACS: Fast, flexible, and free. *Journal of Computational Chemistry, 26*(16), 1701–1718.
Verheul, M., Pedersen, J. S., Roefs, S. P. F. M., & Kruif, K. G. (1999). Association behavior of native β-lactoglobulin. *Biopolymers, 49*(1), 11–20.
Vestergaard, M., Chan, S. H. J., & Jensen, P. R. (2016). Can microbes compete with cows for sustainable protein production - a feasibility study on high quality protein. *Scientific Reports, 6*(1), 36421.
van der Weele, C., Feindt, P., Jan van der Goot, A., van Mierlo, B., & van Boekel, M. (2019). Meat alternatives: An integrative comparison. *Trends in Food Science & Technology, 88*, 505–512.
Yagi, M., Sakurai, K., Kalidas, C., Batt, C. A., & Goto, Y. (2003). Reversible unfolding of bovine beta-lactoglobulin mutants without a free thiol group. *Journal of Biological Chemistry, 278*(47), 47009–47015.
Yan, Y., Seeman, D., Zheng, B., Kizilay, E., Xu, Y., & Dubin, P. L. (2013). pH-dependent aggregation and disaggregation of native β-lactoglobulin in low salt. *Langmuir, 29*(14), 4584–4593.